

Open University of Cyprus

School of Pure and Applied Sciences

Master Degree

Sustainable Energy Systems

Master Thesis



Solar Glare Hazard Analysis of PV Farms Near Airports

Georgios Stavrou

Advisor

Asst.-Prof. Dr.-Ing. Paris A Fokaides

May 2021

Open University of Cyprus

School of Pure and Applied Sciences

Master Degree

Sustainable Energy Systems

Master Thesis

**Solar Glare Hazard Analysis of PV Farms Near Airports
Georgios Stavrou**

**Advisor
Dr.-Ing. Paris A Fokaides**

The present dissertation was submitted for partial fulfilment of the requirements for the degree of Sustainable Energy Systems from the School of Pure and Applied Sciences of the Open University of Cyprus.

May 2021

Περίληψη

Οι ανανεώσιμες πηγές ενέργειας και ειδικότερα οι εγκαταστάσεις φωτοβολταϊκών πλαισίων, κερδίζουν έδαφος στον τομέα της παραγωγής ηλεκτρικής ενέργειας. Είναι πολύ σημαντικό να διασφαλιστεί ότι αυτή η τεχνολογία δεν αποτελεί απειλή για τον άνθρωπο και το περιβάλλον γενικότερα. Η αντανάκλαση της ηλιακής ακτινοβολίας από τις φωτοβολταϊκές εγκαταστάσεις σε σχέση με τα αεροπορικά ταξίδια προσελκύει μεγάλο ενδιαφέρον, όχι τόσο λόγω της συχνότητας των ατυχημάτων, αλλά περισσότερο λόγω της σοβαρότητας ενός ατυχήματος εάν συμβεί.

Με τη διατριβή επιχειρείται να διερευνηθεί η παγκόσμια ανησυχία για την επίδραση της αντανάκλασης από τα φωτοβολταϊκά πάρκα στα αεροπορικά ταξίδια, οι προσπάθειες που έγιναν για τη ρύθμιση της ανάπτυξης των πάρκων αυτών σε διαφορετικές χώρες, να αποδειχθούν ή να αμφισβητηθούν προηγούμενες μελέτες επί του θέματος και να αξιολογηθεί η επίδραση ενός φωτοβολταϊκού πάρκου σε κοντινή απόσταση από το Γενικό Νοσοκομείο Λευκωσίας, σε σχέση με το ελικοδρόμιο του Νοσοκομείου.

Η προτεινόμενη τοποθεσία του φωτοβολταϊκού πάρκου περιγράφεται λεπτομερώς όσον αφορά τα τεχνικά χαρακτηριστικά και τη γεωγραφική θέση. Οι διαδρομές προσγείωσης και απογείωσης των ελικοπτέρων χαρτογραφούνται και εξετάζονται σε σχέση με τις φωτοβολταϊκές συστοιχίες.

Η μεθοδολογία περιλαμβάνει τον προσδιορισμό της θέσης του προτεινόμενου έργου και τον προσδιορισμό των σημείων επηρεασμού ανάκλασης που πρέπει να ληφθούν υπόψη.

Εκτελούνται προσομοιώσεις με συγκεκριμένο λογισμικό και τα αποτελέσματα αξιολογούνται προκειμένου να εντοπιστούν πιθανά προβλήματα αντανάκλασης και να διερευνηθούν εναλλακτικές λύσεις.

Summary

Renewable energy sources and photovoltaic installations in particular, are gaining ground in the power supply sector. It is of great importance to assure that this technology does not pose any threat to humans and the environment in general. Glint and glare reflection from photovoltaic installations with regards to aviation travel draws a lot of attention, not so much because of the frequency of accidents but more because of the severity of one if it occurs.

With the Thesis it is attempted to investigate, the global concern on the effect of glint and glare from Photovoltaic (PV) farms on aviation travel, the attempts made to regulate their development in different countries, to strengthen or contradict existing research and other global perception of glare risks to aviation travel and to assess the effect of a PV farm in close vicinity to Nicosia General Hospital in relation to the Hospital's Helipad.

The proposed location is described in detailed as far as technical characteristics and geographical location. The landing and take-of paths of the helicopter are mapped and are correlated with the photovoltaic arrays.

The methodology includes identification of the location of the proposed project, technical specifications and installation parameters and identification of the receptor points to be considered for glare effect.

Software simulations are executed and the results are assessed in order to identify possible glare issues and investigate mitigation measures and alternatives to the proposed solution.

Acknowledgements

I hereby would like to thank my Advisor, Dr.-Ing. Paris A Fokaides, for all his assistance on the completion of this Thesis and for the opportunity he has given me to perform a hazard analysis on this important issue of glint and glare on aviation travel. In addition to the knowledge and expertise gained on the subject, the results of the assessment can and will be applied towards Nicosia General Hospital's energy management policy and for the benefit of the public in general.

TABLE OF CONTENTS

PAGE

Chapter 1.....	1
Introduction.....	1
1.1 Introduction	1
1.2 Importance of thesis	2
1.3 Objective	3
1.4 Literature review	3
Chapter 2.....	6
Global Regulations and Theory on Solar Reflectance.....	6
2.1 Global Guidance on the Effect of Glare	6
2.2. Theoretical background	8
2.2.1 Effect of Solar Glare on Human Eye.....	8
2.2.2 Reflectivity.....	9
2.3 Photovoltaic phenomenon	11
2.4 Suitability of PV Farms for Airport Applications	12
2.5 Possibility of Occurrence of Glint and Glare	13
2.6 Solar Glare Analysis Tools.....	13
Chapter 3.....	15
PV Farm Configuration.....	15
3.1 Photovoltaic Panels.....	16
3.1.1 Types of photovoltaic panels.....	16
3.1.2 Photovoltaic Panel Efficiency and Power Production.....	17
3.2 Mounting Structures	18
3.2.1 Rooftop installation.....	19
3.2.2 Ground Installation.....	20
3.2.3 Tracking Systems.....	20
3.3 Inverter	22
3.4 Factors affecting Performance of PV installations	22
3.4.1 Environmental factors.....	22
3.4.2 System Factors Affecting Performance.....	23
Chapter 4.....	25
Existing PV Farm Installations.....	25
4.1 Description of existing PV parks near airports.....	25
4.1.1 Narita Tokyo.....	25

4.1.2 Barcelona.....	26
4.1.3 Munich.....	26
4.1.4 Pittsburg.....	27
4.1.5 Fresno.....	27
4.1.6 Athens.....	28
4.2 Description of PV parks near airports in Cyprus	29
4.2.1 Larnaca Airport Photovoltaic Farm Location.....	29
4.2.2 Larnaca PV Farm Technical Characteristics.....	30
4.2.4 Glint and Glare Phenomenon from PV panels.....	32
4.2.3 Glint and Glare Assessment.....	33
4.2.4 Assessment Results and Conclusions.....	36
Chapter 5.....	38
Proposed Project Assessment.....	38
5.4 Description of PV Project.....	40
5.4.1 PV Farm Location.....	40
5.4.2 Nicosia General Hospital PV Farm Technical Characteristics.....	41
5.4.3 Cost Benefit Analysis for PV System installation.....	42
5.4.4 Glint and Glare Assessment.....	42
5.5. Presentation of results and discussion.....	45
5.5.1 Assumptions and Simplifications.....	45
5.5.2 Assessment Results	46
5.5.3 Maximum Annual Energy Production.....	46
5.5.4 Mitigation Measures.....	47
5.5.5 Conclusions	47
References	49
Appendix 1. Larnaca Airport Glare Analysis Results.....	53
Appendix 2. PV Arrays.....	54
Appendix 3. PERC SOLAR CELL PV Panels.....	55
Appendix 4. Photovoltaic Geographical Information.....	57
Appendix 5 – GlareGauge Assessment.....	60

LIST OF FIGURES

Figure 1. Solar Power Plants Worldwide (Air Transport Action Group, 2020).....	2
Figure 2. Impact of light on the human eye (Ho, 2009)	8
Figure 3. Irradiance and effect on human vision (ForgeSolar, 2019).....	9
Figure 4. Effect of sunlight incident angle on reflectance (Forgesolar, 2019)	10
Figure 5. Reflectance with regards to panel surface and tilt angle (Yellowhair, 2015) ..	10
Figure 6. Reflectivity during 24 hours (ForgeSolar, 2019).....	11
Figure 7. Sun’s trajectory in the sky (Innovision, 2019).....	13
Figure 8. Schematic diagram of a PV system (ForgeSolar, 2019)	15
Figure 9. Comparison of polycrystalline (left) and monocrystalline (right) silicon cells (University of Calgary, Energy Education, 2018)	16
Figure 10. Thin film solar panel (University of Calgary, Energy Education, 2018).....	17
Figure 11. Incident Solar radiation as affected by PV panel tilt (Introduction to Photovoltaic System Design, (Balfour, 2011)	18
Figure 12. PV rooftop installation (FAA, 2018).....	20
Figure 13. PV Farm Structures (Balfour, 2011)	20
Figure 14. Fixed, single and twin axis rotational systems (Gevorkian, 2008)	21
Figure 15. PV Modules With Tracking System (Pearsal, 2016)	21
Figure 16. Prologis PV Park (Prologis, 2021).....	26
Figure 17. Pittsburgh Airport Microgrid (Airport Experience News, 2020)	27
Figure 18. Fresno Airport PV farm installation (C&S Engineers, Inc., 2012).....	28
Figure 19. Aerial view of Athens International Airport PV farm installation (Greenair, 2012).....	29
Figure 20. Larnaca Airport and PV farm Location (Nicolaidis & Associates, 2019)	30
Figure 21. Dimensions and Inclination Angle of the Structure and PV Panels (Nicolaidis & Associates, 2019).....	31
Figure 22. Reflectivity of PV Modules and Other Material (ForgeSolar, 2019)	32
Figure 23. Larnaca Airport PV Panels Arrays(Nicolaidis & Associates, 2019)	33
Figure 24. Subtended angle of the sun (Ecoursesonline, 2021)	34
Figure 25. PV array locations, Airtraffic Control Tower and Flight Paths(Nicolaidis & Associates, 2019)	36
Figure 26. Nicosia General Hospital (Google Maps, 2021)	40
Figure 27. Proposed PV Farm Location (Google Maps, 2021).....	40
Figure 28. Helicopter Flight Paths (Cyprus Civil Aviation Department).....	43

LIST OF TABLES

Table 1. PV modules characteristics (Nicolaidis & Associates, 2019).....	31
Table 2. Relative reflectivity of different materials (PagerPower, 2019)	32
Table 3. Simulation Results.....	46

Chapter 1

Introduction

Safety in aviation travel draws a lot of attention, not so much because of the frequency of accidents but more because of the severity of one if it occurs. The thesis attempts to investigate the global concern on the effect of glint and glare from Photovoltaic (PV) farms on aviation travel, the attempts made to regulate their development in different countries and assess the effect of a PV farm in close vicinity to Nicosia General Hospital in relation to the Hospital's Helipad.

1.1 Introduction

Airports are usually located in the outskirts of cities, so that they are far from tall buildings but on the other hand are still in close proximity for convenience in transportation. The surrounding areas are usually left undeveloped so that they do not pose any obstruction to airplane landing and take-off.

This undeveloped land is ideal for the deployment of PV farms because of the large area availability and the low height of nearby development. Apart from that, there is also available space on airport building rooftops.

In addition, airports have high electricity consumption and on-site renewable energy sources (RES) are highly profitable and provide substantial contribution to national goals for RES share in the energy sector. As mentioned in the publication "Bangalore's Airport to Become a Leader in Solar Energy Production" (World's Resources Institute, 2016), *"an airport's electricity consumption, can amount to 100-300 gigawatt-hours (GWh) per year, the same as 30,000 to 100,000 households, or a small city."*

In recent years and with the growing penetration of PV farms in the energy sector, concerns have been raised regarding solar glare hazards in aviation when these farms are developed near airports.

The construction of such farms is gaining ground and Figure 1 is an indication of the large number already in operation worldwide.



Figure 1. Solar Power Plants Worldwide (Air Transport Action Group, 2020)

1.2 Importance of thesis

The importance of this thesis lies in the probable danger which PV farms might pose due to glint and/or glare. In the particular case which will be assessed for the Nicosia General Hospital's Helipad, there is great concern, not only for the safety of the helicopter flights and aviation personnel and passengers but also for the safety of the patients and personnel of the Hospital, the Hospital as a facility and its uninterrupted and continuous operation.

Glint is considered to be an instantaneous light flash while glare is the excessive light from a continuous source. Any surface other than a black body can cause glint and glare. The question which arises is whether or not this light reflected from PV panels, may cause unwanted visual distraction to aviation personnel (pilots, air traffic personnel, Air Traffic Control Tower).

1.3 Objective

The thesis will investigate the theoretical background and the determination of glint/glare occurrence. Existing PV farms will be examined and investigated in relation to the proposed PV farm near Nicosia General Hospital.

With the use of an appropriate software tool, glare assessment of an existing and the proposed PV farm will be carried out. The following will be calculated:

- When and where glare will occur throughout the year for the prescribed solar installation,
- Potential effects on the human eye at locations where glare occurs, and
- An estimate of the maximum annual energy production.

1.4 Literature review

Power production from photovoltaic systems is one of the most developing renewable energy technologies. In his book 'Introduction to Photovoltaic System Design' (2011), John R. Balfour, a United Nations' Committee (International Electrotechnical Committee for Renewable Sources) expert in the photovoltaics area, characterizes the design of Photovoltaic systems as both "*an art and a science*" (Balfour, 2011). The system as a whole does not pose a great difficulty in engineering design but the appropriate matching of parts and subsystems must be carefully selected for an efficient and trouble free operation. This book focuses on the "interrelationship" of these parts in order to design a new high performance system or to improve an existing installation.

Nicola Pearsall, Professor in North Umbria University, Newcastle, and a world-leading expert on photovoltaics, in his book "The Performance of Photovoltaic (PV) Systems" (2016), addresses the power losses and degradation rates which should be accounted for in PV system design. In addition to that, in the book the most common and frequently observed system failure occurrences are summarized with the intent of being prevented.

In Dr Peter Gevorkian's book, "Solar Power in Building Design" (2008), a complete explanation of the photovoltaic sector is presented, starting with the photovoltaic phenomenon and going through the design, economics and environmental contribution of this sustainable technology. With regards to this Thesis, in the book it is very well

explained how the sun's trajectory affects the placement of the PV panels and the efficiency of the system.

"Energy Processing and Smart Grid", is a comprehensive book of the way different sources and loads are interconnected through power electronic devices, by Dr James A. Momoh, a Professor of Electrical Engineering and Computer Science with Howard University, USA, and a Fellow at the Institute of Electronics and Electrical Engineering (IEEE) and a Distinguished Fellow at the Nigerian Society of Engineers (NSE). In his book, Dr. Momoh, elaborates on renewable energy sources and photovoltaics in particular, energy storage, power conversion (DC to Ac and vice versa), inverters and converters, power metering and the way these individual parts are connected to a power supply system.

The U.S. Federal Aviation Administration of the U.S. Department's of Transportation, has published a number of important documents with regards to aviation safety which most of them are used globally as reference, as follows:

- "Technical Guidance for Evaluating Selected Solar Technologies on Airports" (2018). The purpose of this Guidance is to assure that any solar exploitation technologies deployed on or near airport space, comply with regulations, or in the absence of that, assure that solar developments do not pose any danger to aviation flights and any other personnel involved (pilots, air traffic controllers, or airport operations). This report also presents case studies of airport PV installations (Denver International, Fresno Yosemite International, Albuquerque International, Sunport).
- "ORDER JO 7400.2M - Procedures for Handling Airspace Matters", (2019). This publication covers a complete list of procedures and programs which can be present in airport facilities and the necessary precautions or actions to be taken regarding these procedures. This publication also includes the boundaries which are considered aviation space within which glint and glare must be evaluated regarding their effect on aviation flights.
- "Interim Policy 78 FR 63276, FAA Review of Solar Energy System Projects on Federally Obligated Airports" (2013). This policy stresses the importance and enforces the use of Solar Glare Hazard Analysis Tool (SGHAT), a tool which is

designed to investigate if a PV installation will have any effect or potential threat to a nearby airport facility or aviation flights in the area. This is the tool which is used in the present Thesis.

“Aviation Benefits Beyond Borders”, is a website of the commercial aviation industry which aims to promote economic growth, social development and environmental efficiency and sustainability in the aviation sector. This is represented by the Geneva-based Air Transport Action Group.

Dr Clifford K. Ho of Sandia National Laboratories, with Cheryl M. Ghanbari and Richard B. Diver, (2009), issued the paper “HAZARD ANALYSES OF GLINT AND GLARE FROM CONCENTRATING SOLAR POWER PLANTS” which also applies on PV power plants, on the effect of glint and glare as a potential hazard or distraction for motorists, pilots, and pedestrians. This publication also reviews the “physiology, optics, and damage mechanisms” with regards to solar radiation and introduces new metrics for temporary flash blindness, which is possible to take place at lower values of radiation than the ones resulting in permanent eye damage.

ForgeSolar is the official developer of the GlareGauge, the most known and used solar glare analysis tool. The company maintains a website with instructional assistance on the use of the tool (<https://www.forgesolar.com/help/>) as well as more general information on solar radiation and on transmittance effects and glint and glare impacts (<https://www.forgesolar.com/static/docs/yellowhair-2015-asmt-pv-surf.pdf>).

The Solar Trade Associations (STA) (2016), is an association of companies in the production and installation industry of solar systems in the United Kingdom. Their main goal is to promote solar energy technology with a high level of quality and support. STA issues solid scientific publications towards their goal, among which the “*Impact of solar PV on aviation and airports*”, with important analysis on glare assessments.

Chapter 2

Global Regulations and Theory on Solar Reflectance

The theory on solar light reflectance has been studied and has been well documented over the years. The regulation of PV farm deployment is still under development.

2.1 Global Guidance on the Effect of Glare

The effect of glare on aviation travel, even though it is gaining global attention due to the increasing number of PV farms near airports, is not regulated to a great extent. The following are a number of countries where efforts have been made to deal with the matter so as to assure that PV installations do not pose a threat to flights and the surrounding environment.

- United States of America

The Federal Aviation Administration (FAA) of the United States is the Body which dealt the most with the effects of glare. As mentioned in the Literature Review in Paragraph 1.4, FAA issued a number of Orders among which the “Technical Guidance for Evaluating Selected Solar Technologies on Airports”. This is considered globally to be the most complete guidance document on the effects of glare and which sets procedures to approach the whole matter. The guidance starts with the basics of PV theory and design, goes through the planning and siting of the PV farm, covers the safety requirements regarding aviation and Environmental Standards and even goes into the economic viability and financing of the PV project.

FAA, under a separate Interim Policy Document, mandates the use of the Solar Glare Hazard Analysis Tool (SGHAT), to carry out glint & glare assessments of PV installations.

This tool is a product of the research facility “Sandia National Laboratories” of the US Department of Energy. Currently, this is the only tool which carries FAA approval to be used for assessing PV glare with regards to aviation travel.

- United Kingdom

United Kingdom is a country where PV installations have been deployed quite a few years back and there have been formal attempts to address the issue of glint and glare and their effect on aviation. The U.K. Civil Aviation Authority (CAA) has issued relevant guidance since 2002, with revisions in 2010 and 2020 regarding solar installations near airports within fifteen kilometers radius. In this guidance (CAA INTERIM GUIDANCE, 2010), it is mandated that concern should be taken to “*provide safety assurance documentation regarding the full potential impact of the PV installation on aviation interests.*” Apart from this obligation arising from the guidance, there is not a specific methodology proposed to the PV farm developer or owner to be followed. Instead, reference is given to the FAA Technical Guidance, as the basis to be followed for the PV farm glare assessment.

- Republic of Ireland

In the Republic of Ireland, where PV farms are also gaining ground as an alternative, renewable source of energy, the Sustainable Energy Authority of Ireland (SEAI) (2016), has also issued the guidance “Planning and Development Guidance Recommendations for Utility Scale Solar Photovoltaic Schemes” . This guidance also calls for glare assessments for large PV solar parks but it does not provide any new research or methodologies. Instead, it also references the FAA Technical Guidance.

- Germany

In Germany, The Federal Ministry of the Environment (2014), issued light guidelines (LichtLeitlinie) which classify glare in the emissions category, along with noise and odor pollution. The acceptable level of glare according to these light guidelines is 30 minutes in one day or 30 hours in one year. It is further defined that glare has harmful effect if the angle between the reflective surface and the sun is more than 15 degrees. According to the local regulations, assessment of PV farms must follow these guidelines.

2.2. Theoretical background

Sunlight reflected from PV panels, can cause glint and glare (from now on both referred to as “glare”), as already mentioned. Glare, under certain conditions can cause temporary loss of vision, or flash blindness. The term “flash blindness”, or “afterimage” is defined by the U.S Department of Transportation (ORDER JO 7400.2M - Procedures for Handling Airspace Matters), as “a temporary visual interference effect that persists after the source of illumination has ceased”. It is thus of primary importance to investigate whether or not these “certain conditions” are present when designing a PV farm near an airport.

2.2.1 Effect of Solar Glare on Human Eye

The impact of light entering the human eye, is demonstrated in figure 2 below. Light goes through the cornea and passes to the pupil. Light rays converge behind the lens (nodal point). The image defined by the light rays is then turned upside down and its projection falls to the retina. “Potential damage to the eye depends on a number of factors including the source radiance, source angle (size and distance to eye), duration of exposure, and wavelength” (Ho, 2009).

The perception of light from the eye depends on the intensity per unit area of the light, usually expressed in cd/m^2 (candela per square meter), which is defined as the luminance of light.

Impact of Light Entering the Eye

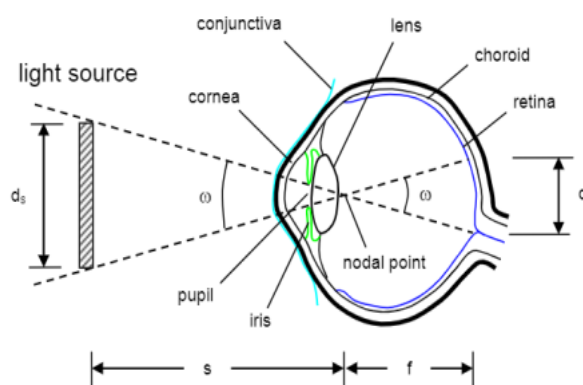


Figure 2. Impact of light on the human eye (Ho, 2009)

Another term used to measure light intensity is the irradiance, which is the power (or flux) of light per unit area measured in watts per unit area. Luminance and irradiance are directly proportional. Figure 3 below denotes the spectrum of irradiance where eye damage or effect occurs with regards to the light source angle.

Potential Ocular Impacts

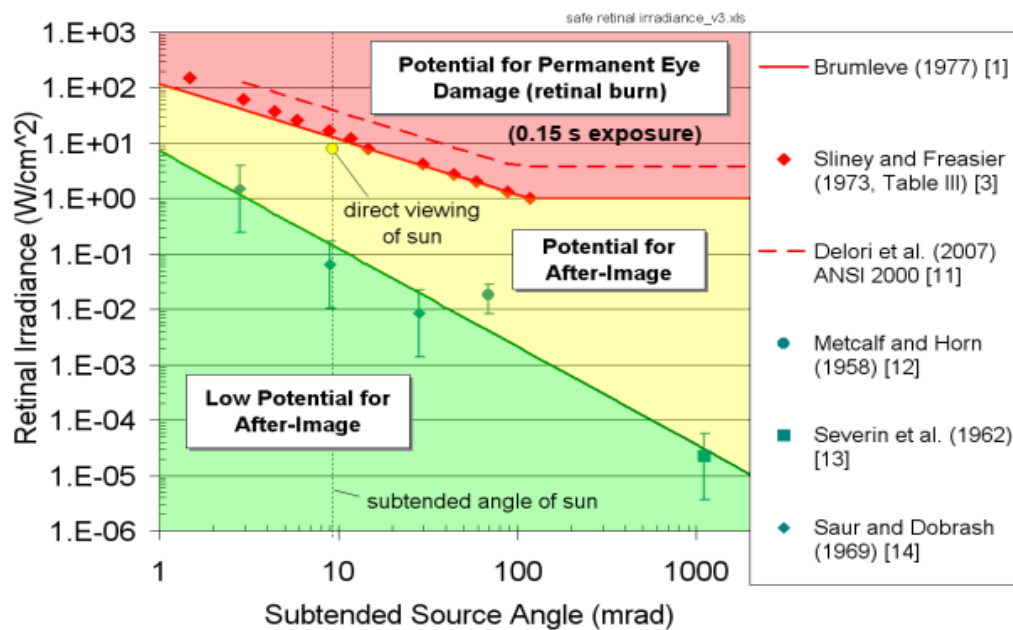


Figure 3. Irradiance and effect on human vision (ForgeSolar, 2019)

Eye damage can occur within the red area of Figure 3, while the potential of afterimage is low in the green area and higher in the yellow area. Afterimage is also defined as the “reverse contrast shadow image left in the visual field after an exposure to a bright light that may be distracting and disruptive, and may persist for several minutes” (U.S Department’s of Transportation, 2019).

2.2.2 Reflectivity

In theory, light reflected from PV farms can cause visual interference to people. It has been proven that solar irradiance with magnitude of 7 W/m² could cause afterimage effect, which can have a 4-12 seconds duration (Ho, 2009) . It should be noted that solar irradiance has typical values of 800 to 1000 watts per m².

Reflectivity depends on the following factors:

- **PV Panel Position Relative to the Sun**

The PV panel tilt angle plays a major role in the reflectance of the panel. Figure 4 below indicates that the bigger the incident angle is, the higher the reflectivity is.

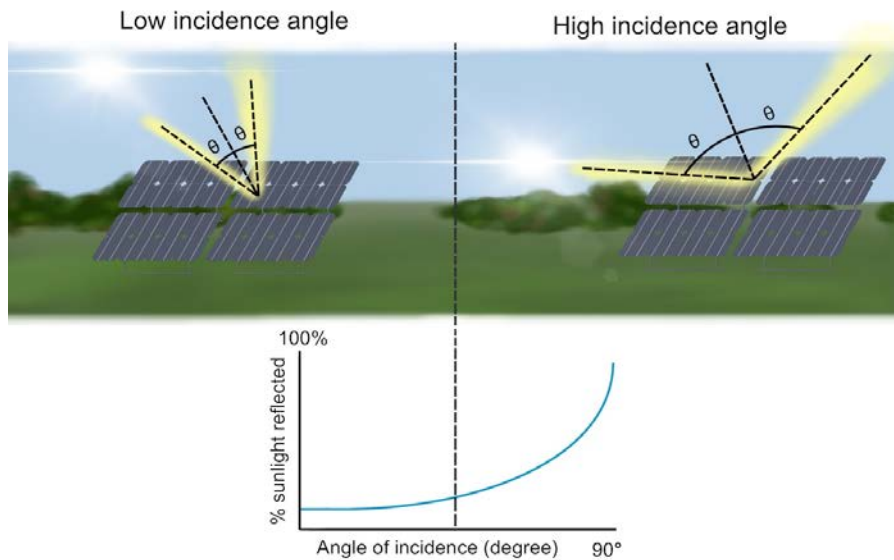


Figure 4. Effect of sunlight incident angle on reflectance (Forgesolar, 2019)

- **PV Panel Construction Material**

The panel material has a very significant effect on the reflectance. By treating the panel surface with antireflective coatings and textured surfaces, the reflectance can be minimized as shown in figure 5 below.

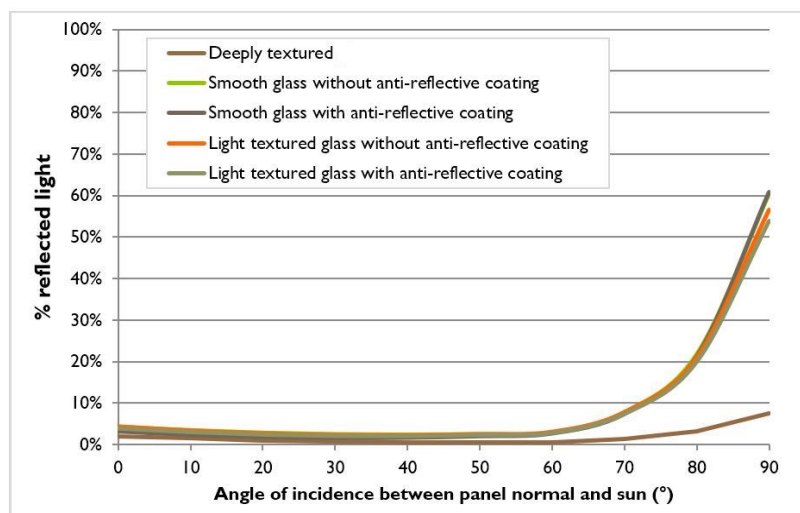


Figure 5. Reflectance with regards to panel surface and tilt angle (Yellowhair, 2015)

● Direct Normal Irradiance at the Specific Site at Midday

Reflectivity is, of course, directly related to the solar irradiance at the area under examination. Following, is an example for a US location showing the irradiance over 24 hours.

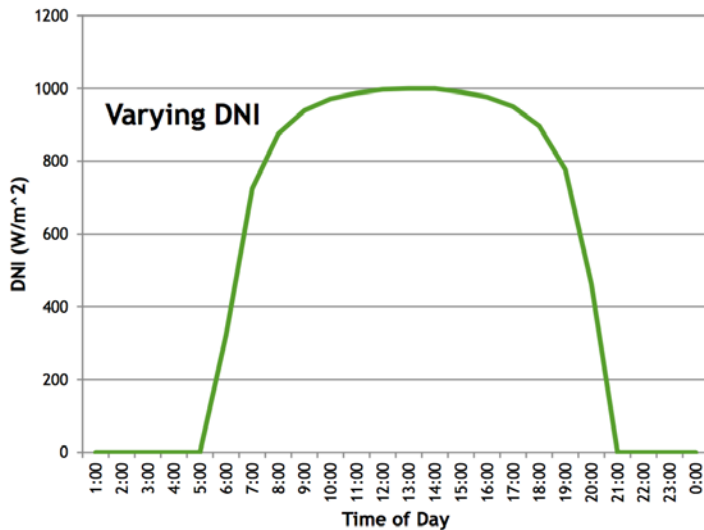


Figure 6. Reflectivity during 24 hours (ForgeSolar, 2019)

2.3 Photovoltaic phenomenon

A photovoltaic cell is a device which converts solar light into electricity. It is made of a semiconductor material and it is usually no bigger than 4 human hairs and it produces up to 2 watts (U.S Department of Energy, 2021).

A photovoltaic panel (or module) consists of a number of photovoltaic cells bonded in chains and held together in-between materials such as glass and plastic in order to be protected. Typical photovoltaic panel outputs range from 250 watts to 400 watts.

Solar light reaching a PV cell, can either go through the cell or it can be reflected or it can be absorbed. PV cells are made of materials which have better conductivity than insulating materials but not as good as conductive materials such as metals. For this reason the PV cell materials are considered to be semiconductors.

Exposure of a semiconductor to solar light, transfers energy to electrons, the negatively charged ions in the material. This transfer of energy creates a flow of electrons, same as

electricity. This flow of electrons, or current, is obtained through the metal contacts which appear like grid lines on a PV panel. This is known as the photovoltaic phenomenon.

2.4 Suitability of PV Farms for Airport Applications

Photovoltaic technology is considered today to be the most appropriate source of onsite power generation application for Airports with *“the best cost-benefit ratio of the solar power alternatives”* (FAA, 2018).

The main advantages of the PV technology are the following:

i. It is proven to be more *“cost-effective”* (FAA,2018), for smaller applications such as Airports when compared to larger installations connected to the grid.

ii. The PV panels have low profile and can be installed in different modules making them suitable for installations on separate buildings roof tops since they do not protrude high in the sky posing danger to aviation flights.

iii. By design the PV panels absorb solar radiation instead of reflecting it, minimizing the risk of danger arising from glare.

iv. They are not suitable for wildlife habitats which would be considered danger to airplane flight.

v. Does not produce electromagnetic pulses which could interfere with airplane instruments and aviation radars.

vi. Does not produce air column movement which would pose danger to flights

In addition to the above, PV technology, has the following advantages:

- a) Requires very little maintenance and upkeep costs are very low.
- b) Can be upgraded very easily by adding additional PV arrays.
- c) Malfunction in one array does not affect the whole system due to its modular design.
- d) Can be used in replacement of other building materials such as parking lot roofing, minimizing building costs.
- e) During the summer months it has the higher production when the demand is also higher.
- f) They are very reliable in operation and have a long lifecycle, up to 25 years.

- g) Environmentally friendly in operation. It does not require any fuel to operate and does not produce pollutants or noise.

2.5 Possibility of Occurrence of Glint and Glare

The occurrence of glint and glare is possible under certain conditions. Taking as an example the trajectory of the sun, from the moment it rises from the east until it sets in the west, it follows an arc in the sky in the south as it is shown in figure 7 below.

Depending on the season, the sun's elevation angle differs, being much higher in the summer months compared to the winter months. At any given time the sun's radiation is reflected on the PV panels in the opposite direction of the sun. This reflected radiation, after a certain elevation angle, does not affect any receptors located on the ground. These receptors are usually only affected by glint or glare in the morning and the evening hours. When it comes to aviation travel though, glint and glare can occur at any time during the day and for this reason it is very important to carry out a glint and glare assessment for any PV farm installation which is close to Airports.

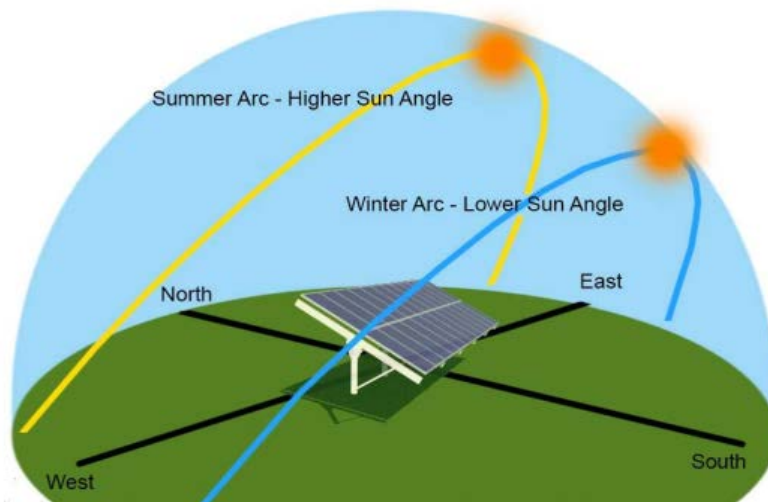


Figure 7. Sun's trajectory in the sky (Innovision, 2019)

2.6 Solar Glare Analysis Tools

A number of different tools have been developed for the determination of glare occurrence. Sandia National Laboratories Center, a U.S. Federally Funded Research and Development Center (Sandia National Laboratories, 2020), has developed the following relevant tools:

- Solar GlareGauge Hazard Analysis Tool
- Tower Illuminance Model
- Empirical Glare Analysis Tool
- Analytical Glare Estimation Tool
- Glare intensity plot
- PHLUX Mapping Analysis Tool
- Reflectivity Calculator Tool

For the project in question, the Solar GlareGauge Hazard Analysis Tool will be used.

The importance of the use of the above mentioned tool is clearly confirmed by its compulsory use *“for any proposed solar energy system located on a federally-obligated airport”*, according to the U.S. Department of Transportation, Interim Policy 78 FR 63276, 2013.

This particular tool incorporates Google Maps where one can draw a virtual PV farm on a selected location. Geographical information is automatically provided along with sun position and vector calculations. The user enters information on orientation and tilt angle of the photovoltaic panels, reflectance, direct normal irradiance and ocular specifications. If, according to the tool’s results, substantial glare occurrence exists, design data are recalculated using the tool to establish the optimum PV array configuration which will yield the maximum energy production without glare present.

Chapter 3

PV Farm Configuration

The deployment of a PV farm requires proper design and understanding of the correlation of the different parts and subsystems. Also, the designer should be aware of the factors which affect the performance of the system and these should be taken into consideration.

Photovoltaic systems are composed of a number of different components and subsystems. The main components for a typical PV grid connected system are the following:

- PV panels
- PV panels mounting structure
- Tracking system (optional)
- Inverter

The following figure demonstrates the complete schematic diagram of a PV system.

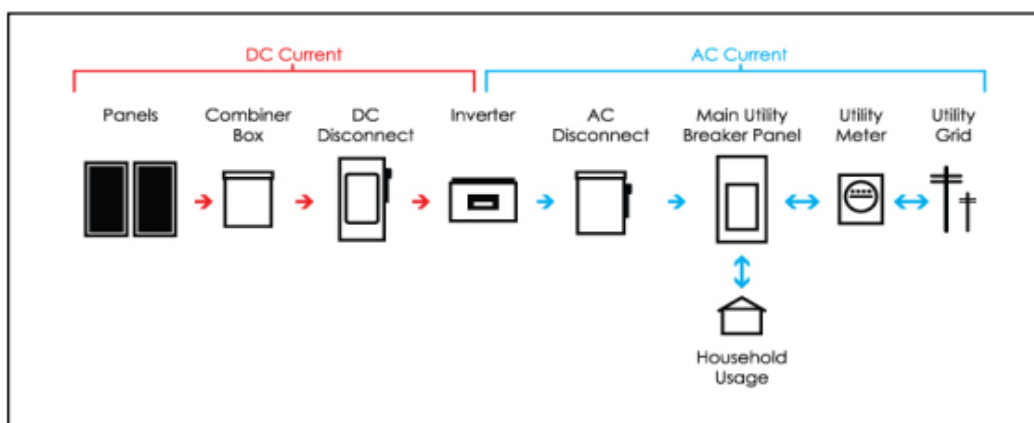


Figure 8. Schematic diagram of a PV system (ForgeSolar, 2019)

3.1 Photovoltaic Panels

The PV panels are the main component of the system since it is the power producing subsystem. Different PV panels exist and it is very important to select the appropriate type which suits the application.

3.1.1 Types of photovoltaic panels

The main PV panel construction types or technologies are monocrystalline panels, polycrystalline panels and thin film panels.

- Monocrystalline panels are constructed from single silicon crystals, formed from silicon after being melted. This type of PV panel is the most efficient with efficiencies ranging from 13% to 16%. It is though the most expensive due to the single crystal manufacturing process.
- Polycrystalline panels are constructed from many smaller silicon crystals. These panels are less expensive but have lower efficiencies ranging from 11% to 14%. These are the most commonly used PV panels with a market share of approximately 70 % (Peake, 2018). Figure 9 below shows the monocrystalline and polycrystalline panels in comparison.

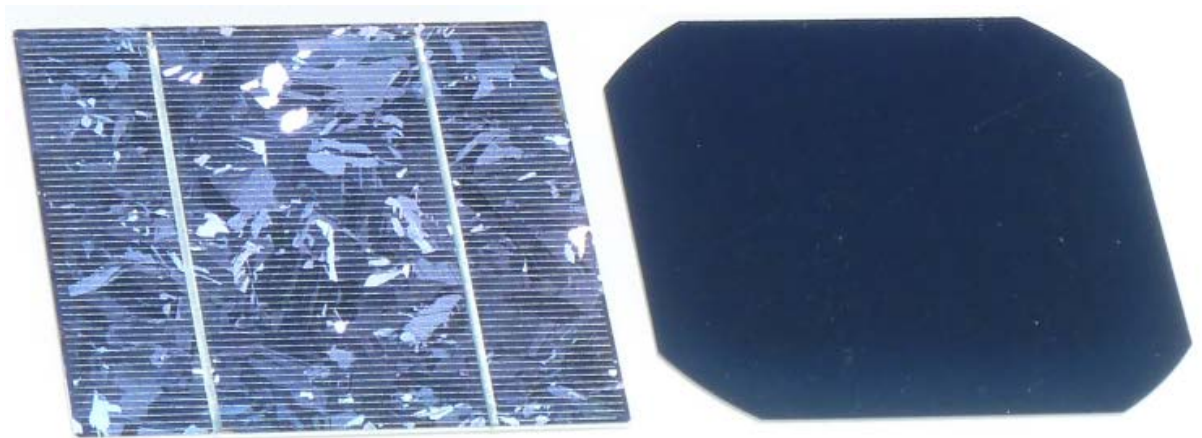


Figure 9. Comparison of polycrystalline (left) and monocrystalline (right) silicon cells (University of Calgary, Energy Education, 2018)

- The third more common type of PV panel is the thin film type which is constructed as the name implies in a flexible thin film from either silicon, copper indium gallium diselenide (CIGS) or cadmium telluride (CdTe) (University of Calgary,

Energy Education, 2018). This type of PV panel is much less expensive as it requires less than 1% material needed for a monocrystalline cell. Their efficiency is also less ranging from 6% to 8% and for this reason require a lot more surface area and installation space to produce the same amount of power as the other PV panel types. Figure 10 below shows an example of a thin film PV solar panel.



Figure 10. Thin film solar panel (University of Calgary, Energy Education, 2018)

3.1.2 Photovoltaic Panel Efficiency and Power Production

The efficiency of a panel is considered to be the power produced from the panel as electricity, divided by the solar light energy which shines on the panel. PV panels of different construction technology and materials, have varying efficiencies. These efficiencies range from 6% to 20% (FAA, 2018). These efficiencies are known to be minimized by approximately 05%/year due to material fatigue and wear.

It is worth considering that the efficiency of the panel increases as its temperature increases but only up to the ideal temperature of 25° C (FAA, 2018). With temperatures rising over the ideal temperature, the efficiency begins to drop. Actually, the decrease in power amounts to 5% per 10°C over the ideal temperature.

Following is an example for the power production of a PV panel. Considering the above efficiency decrease (5% per 10°C over the ideal temperature) , the power produced from a 315w PV panel at a temperature of 35° C, during 7,13 hours of sunlight availability would be

$$(315w \times 0,95) \times 7,13hrs = 2,134 \text{ kWh}$$

3.2 Mounting Structures

The PV panels need to be mounted on a structure which serves specific purposes. This structure must be able to withstand the local weather conditions and must be strong enough to carry the weight of the entire system.

The mounting structure should provide the panel orientation and the optimum panel tilt which are required to produce the maximum electricity production for a certain geographical point. For PV installations in the northern hemisphere, the optimum orientation is true south and in the southern hemisphere the orientation should be true north (University of Calgary, Energy Education, 2018). The optimum inclination should be at an angle equal to the local geographical latitude (Gevorkian, 2008). Neither horizontal nor vertical positioning of the panels is considered optimal despite the simplicity of the mounting structure. Figure 11 below shows clearly the difference in incident radiation received by the same panel in the horizontal, vertical and tilted positioning.

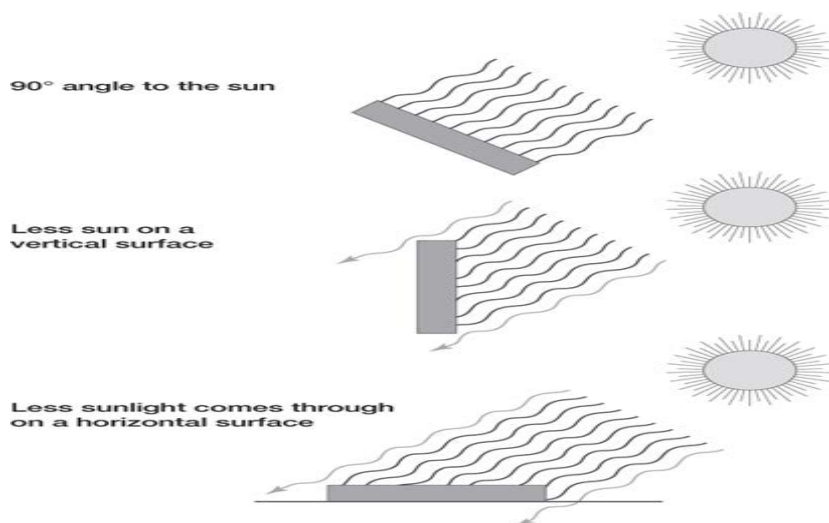


Figure 11. Incident Solar radiation as affected by PV panel tilt (Introduction to Photovoltaic System Design, (Balfour, 2011))

Mounting structures can be located on rooftops, directly on the ground or even at elevated structures providing shade over parking lots. These structures can be stationary or have single or twin axis rotation capabilities. The mounting structure represents a major cost percentage to the whole system and it should be carefully selected and designed. Nicola Pearsall in his book, "The Performance of Photovoltaic (PV) Systems", explains in detail the factors which need to be taken into consideration before a decision is reached. These factors are the following:

- Initial Procurement Cost comparison

Rooftop mounting saves on infrastructure since existing roof can be used for anchoring the PV mounting structure

- Maintenance Costs

Rooftop mounting has higher cost for panel cleaning maintenance but ground mounting should account for cleaning the area from weeds and trees growing in-between PV panels. As elaborated in the book “Advanced Photovoltaic Installations” by Balfour, 2011, especially near airports and highways, PV panel arrays will require frequent cleaning with high pressure water.

- Running Costs

Stationary structures have limited running costs as opposed to tracking system structures which consume electricity in order to run.

- Load Calculations

Load calculations should account for weather conditions such as wind and snow load.

- System Degradation

Roof mounting as compared to ground mounting structures, in hot climates are prone to higher degradation rates which affect system efficiency and could be up to 1% per year.

3.2.1 Rooftop installation

Rooftop installations are usually considered ideal for PV applications, especially if there is not any shading from nearby buildings or other obstacles. Roof structural supports can substitute to an extent the PV system support structure making the installation more cost effective. Should the roof orientation and inclination be appropriate for the certain geographical location, as explained at the beginning of this paragraph, then the only consideration would be the load calculation for the weight of the system and other weather concerns (snow, wind, hurricanes, etc.). Airports usually have large rooftop areas which can be utilized for PV installations without sacrificing valuable land space which could be put in other uses. Usually, rooftop installations tend to be more suitable for smaller PV farms than ground mounted PV installations. Figure 12 below shows an example of a rooftop installation.



Figure 12. PV rooftop installation (FAA, 2018)

3.2.2 Ground Installation

The simplest PV installation is deployed on the ground. Main requirements are a flat level area and south orientation without shading. Once the appropriate area is selected, the stability of the system must be established so as to have a long lasting installation which will not suffer from destabilization and efficiency losses.

Ground applications include directly on the ground level installations and installations on elevated structures to provide car shading (Figure 13) as shown below.



Figure 13. PV Farm Structures (Balfour, 2011)

Ground installations favor larger scale projects to be more economical, as long as the land used for the installation does not have any other more profitable opportunities for development.

3.2.3 Tracking Systems

More complicated mounting structures include single and twin rotational systems which have the ability to alter the orientation and the tilting of the panels during the day to follow the sun's path in order to maximize the power output, thus the efficiency of the system. One directional movement of the panels is perpendicular to adjust for the sun's position relative to the season and the other movement is horizontal to track the sun's

movement throughout the day. If the system employs one of the movements is called a single axis system and if it employs both it is a twin axis system. The purpose of the rotation is to have the panels facing the sun perpendicular at all times. Examples of the fixed, single and twin axis rotational systems are shown in figure 14 below.

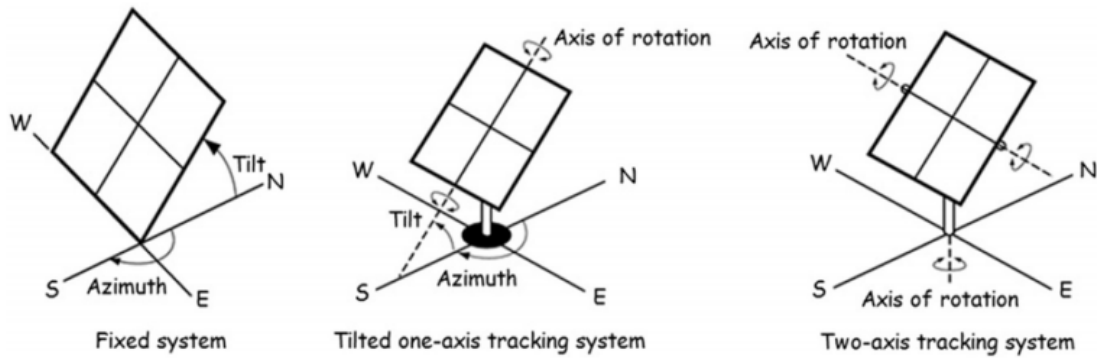


Figure 14. Fixed, single and twin axis rotational systems (Gevorkian, 2008)

These tracking systems have substantially higher initial and maintenance costs which should be weighed against the output benefit before a certain system is selected.

An example of a PV tracking system is shown in figure 15 below.



Figure 15. PV Modules With Tracking System (Pearsal, 2016)

Solar tracking systems are more suitable in countries where sunlight hours are more in one day, such as Cyprus. It is estimated that tracking systems can have 10% up to 40%

power increase over stationary systems. This benefit must be weighed against the extra installation, repair and maintenance costs before a decision is reached.

3.3 Inverter

The electrical current produced by the PV panels is directed in a combiner box and it is then supplied to the inverter. An inverter is a converter which changes *“a DC input voltage to a symmetrical AC output voltage of desired magnitude and frequency”* (Momoh, 2018). The inverter is the part of the system where the 30-40V direct current (DC) produced by the PV panels is converted to 220-240V alternating current (AC). Losses in the inverter part of the system range from 2% to 15% and it is of great importance to make the right selection in order to have the maximum possible overall efficiency. The system also incorporates a breaker panel necessary to protect the system from current surge and short circuits. If the electricity is supplied to the grid, a utility meter is also present to calculate the onsite consumption of power and the power supplied to the grid.

3.4 Factors affecting Performance of PV installations

A number of factors affect the performance of PV power generation. These factors fall under the categories of environmental factors and system factors as follows:

3.4.1 Environmental factors

The environmental factors which affect the efficiency and performance of photovoltaic systems are mainly solar irradiance, temperature, debris accumulation and shading.

i. Solar Irradiance

Solar irradiance is the sun's power per unit area. This power is directly related to the output power of PV panels. For this reason, a panel's power output is also directly related to the geographical location of the PV farm and the location of the sun throughout the day and throughout the year.

ii. Environmental Temperature

The PV panel's temperature, which is directly affected by the environmental temperature, has the greatest effect on the system's performance. As it has already been explained in paragraph 3.1.2, if temperature rises over the ideal temperature of 25° C, the efficiency drops 5% per 10°C.

iii. Debris accumulation

Debris such as dirt, dust and leaves has a significant power reduction on the PV panel. According to various studies on the matter, it was concluded that relative to the geographical or topography location and the type and size of dust in an area, a 7% to up to 65.8% reduction in PV panel efficiency may occur (M.M. Fouada, Lamia A. Shihatab, ElSayed I. Morgan,). These studies indicate the importance of regular maintenance and cleaning of the PV panels.

iv. Shading

Shading of the PV panels is another environmental factor with negative effect on PV performance. Shading affects the whole panel efficiency and not only the cells of the panel under shade, since the cells are connected in series. This considering, even poles and trees can affect the performance of the system and definitely tall buildings with much higher shading density. Studies have shown that even with a 5%-10% shading, the system might suffer for up to 80% performance reduction (M.M. Fouada, Lamia A. Shihatab, ElSayed I. Morgan, 2017).

3.4.2 System Factors Affecting Performance

Apart from environmental factors, various system factors or individual parts also have an effect on the performance of the whole system. These are mainly the PV panel's characteristics, the inverter efficiency and the inclination and orientation of the panels.

i. PV panel's characteristics

The panel' characteristics which affect performance is the technology and material construction as explained in paragraph 3.1.1 and the energy conversion efficiency of the panel. The conversion efficiency is given by the manufacturer and it is related to the *"rated power of the PV panel, the surface area of the panel and the solar irradiance"* (M.M. Fouada, Lamia A. Shihatab, ElSayed I. Morgan, 2017).

ii. Inverter Efficiency

The inverter is another part which has an effect on system performance and efficiency. This was already discussed in paragraph 3.3.

iii. PV panels inclination and orientation

The inclination and orientation of the PV panes are two of the most significant system parameters affecting the performance and efficiency of the system. As explained in paragraph 3.2.3 on tracking systems, ideally, the panels should be facing the sun perpendicularly at all times. As a general guideline, especially in fixed angle systems, the ideal tilt angle should be equal to the geographical latitude of the installation. It should be noted though that the *“tilt angle deviates approximately +15° from the latitude angle in winter and about -15° of the latitude angle in summer”* (M.M. Fouada, Lamia A. Shihatab, ElSayed I. Morgan, 2017). Kaddoura TO, Ramli MA and Al-Turki YA with their report *“On the estimation of the optimum tilt angle of PV panel in Saudi Arabia, 2016”*, have proven that with 6 yearly adjustments of tilt angle, *“99.5% of solar radiation can be harvested”*.

Chapter 4

Existing PV Farm Installations

Due to the growing concern on the effect of PV farms near Airports, it was deemed necessary for the purposes of the Thesis to investigate the deployment of other PV installations.

4.1 Description of existing PV parks near airports

For the reasons explained in Chapter 1, PV farms near airports already exist throughout the world. Examples of such PV parks have been constructed at the following locations:

- Narita Tokyo
- Barcelona
- Munich
- Pittsburgh
- Fresno
- Athens
- Larnaca

The increasing number of PV parks to supply electricity to airports, denotes the importance of the particular application and the subsequent importance of this thesis. Following is a brief description of the above installations with the exception of the Larnaca PV farm, where a more detailed description is given on the glint and glare assessment of the PV farm.

4.1.1 Narita Tokyo

The photovoltaic park is located at the South of the airport as shown in Figure16 below.

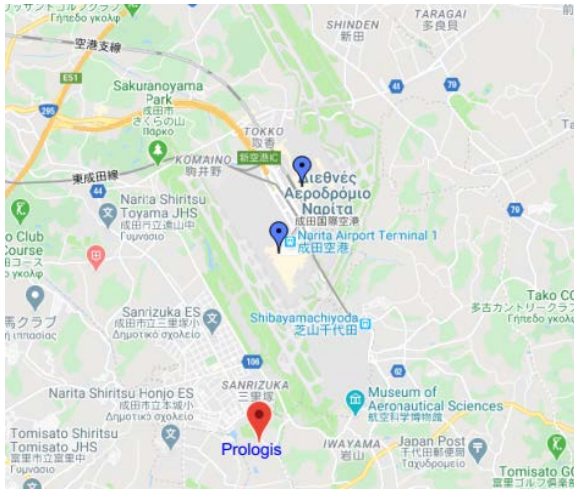


Figure 16. Prologis PV Park (Prologis, 2021)

The PV array is installed on the rooftop of a Prologis warehouse. Prologis is an international company specializing in the industrial real estate and logistics services. Alongside their main operation, Prologis makes use of their warehouse rooftops for PV farm installations.

The PV farm has the following characteristics:

- Installed power 18,847 kWp
- Electricity production per year 500,000kWh
- Average reduction of CO2 emissions per year 8,139,428 kg
- Equivalent to energy use in number of households 4,926

4.1.2 Barcelona

The PV installation at Barcelona Airport (WSP Global Inc., 2021), is an ongoing process. It started in 2003, and it was, at the time, the largest PV airport installation. The panels were installed on the airport's rooftop and had the following characteristics:

- Installed power 450 kWp
- Electricity production per year 500,000kWh
- Average reduction of CO2 emissions per year 500 tons
- Equivalent to energy use in number of households 200

4.1.3 Munich

The PV Park in Munich Airport (Munich Airport, 2019) was completed in 2018 and it is located on top of the parking area. The PV Parks capacity is as follows:

- Installed power 750 kWp
- Electricity production per year 800,000kWh
- Average reduction of CO2 emissions per year 500 tons
- Equivalent to energy use in number of households 350

4.1.4 Pittsburgh

At Pittsburgh Airport, the intent is to install a PV Park of such capacity (as part of an onsite Microgrid), to be completely self-sufficient as far as electricity is concerned. The Airports electricity consumption is 14MW and the PV Park will have a capacity of 2.5MW. The additional capacity will be provided by the Microgrid as shown in Figure 17 below incorporating five natural gas-fueled generators.



Figure 17. Pittsburgh Airport Microgrid (Airport Experience News, 2020)

4.1.5 Fresno

The PV farm has been constructed on a 9.5acres plot of the airport's land which didn't have any other development potential.

The 11,700 panels have the ability to move hydraulically following the sun's position for optimum production.

The farm's capacity is 4.2MW and it covers 58% of the electricity consumption of the airport.

Following is an aerial view of the installation.



Figure 18. Fresno Airport PV farm installation (C&S Engineers, Inc., 2012)

4.1.6 Athens

Athens International Airport, incorporates the largest airport PV farm installation. The project started in July 2004, with a pilot installation of 7,500 kWh capacity and was completed in 2012 with a PV farm of 8MW capacity. The farm is developed on airport land.

Following are the PV farm's characteristics:

- Installed power 8MWp
- Electricity production per year 11,000,000kWh
- Average reduction of CO₂ emissions per year 10,000 tons
- Equivalent to energy use in number of households 350

Following is an aerial view of the PV farm in Athens.



Figure 19. Aerial view of Athens International Airport PV farm installation (Greenair, 2012)

4.2 Description of PV parks near airports in Cyprus

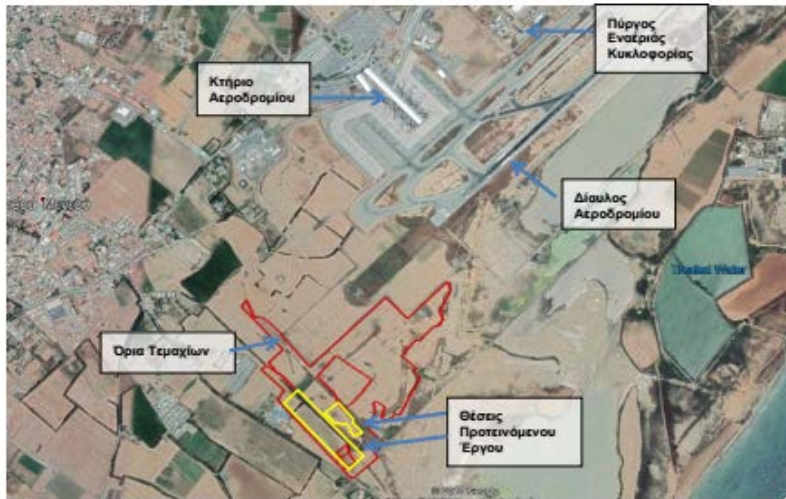
The official airports in Cyprus are located in Larnaca and Paphos. Both airports are operated by Hermes Airports Ltd. The company intends to install a 3.5 MW farm in Larnaca Airport and a 1.1 MW farm in Paphos Airport. The installations aim to cover 25% and 30% of consumption for Larnaca and Paphos Airports respectively.

The Larnaca installation is in progress even though it has been delayed when it had to be partially moved to preserve fields with *Orphys kotschyi* orchids and *Carchysscabra* plants (Balkan Green Energy News, 2020). It is expected to be completed by the end of current year.

Following is a description of the proposed installation of the PV farm near Larnaca Airport. The following information is depicted from a glare assessment carried out by Nicolaides & Associates (2019) for the licensing purposes of the PV farm.

4.2.1 Larnaca Airport Photovoltaic Farm Location

The PV farms is located 4km west of the city of Larnaca. It is at 1.5km distance from the Airport building and 2.1km distance from the Airport traffic control tower. An aerial photograph of the PV farm location is shown in figure 20 below.



Εικόνα 4-1: Περιοχή Μελέτης

Figure 20. Larnaca Airport and PV farm Location (Nicolaidis & Associates, 2019)

4.2.2 Larnaca PV Farm Technical Characteristics

The project involves a PV farm of 3.5MW capacity. The PV farm will be supplying power to the Airport and any surplus to the Cyprus Electric Authority power grid.

i. PV modules

The installation will include 11290 PV modules of 315W capacity each. The dimensions of the panels are 1650 x 992 x 35 mm. The support structure will be of the fixed poles type without rotational capability. The technical characteristics are shown in table 1 below (Nicolaidis & Associates, 2019).

STP 310S- 20/Wfs (MC4_270) SPECIFICATIONS	
All Black Anti-Reflection Coating	
Electrical Data	
Maximum Power (Pmax)	310W
Maximum Power Voltage (Vmp)	33.1V
Maximum Power Current (Imp)	9.37A
Open-circuit Voltage (Voc)	40.2V ± 5%
Short-circuit Current (Isc)	9.87A ± 5%
Module Efficiency STC (%)	18.9%
Operating Temperature(°C)	-40°C~+85°C

Maximum system voltage	1500VDC (IEC)
Maximum series fuse rating	20A
Power tolerance	0 ± 5W
Temperature coefficients of Pmax	-0.39%/°C
Temperature coefficients of Voc	-0.34%/°C
Temperature coefficients of Isc	0.060%/°C
Nominal operating cell temperature (NOCT)	42±2°C
Mechanical Data	
Width	1650 mm
Length	992 mm
Depth	35 mm
Weight	18.3 kg
Total Area	1.63m ²
Frame	Anodized Aluminum Alloy
Connectors	MC4 compatible
Warranty and Qualifications	
Cell Type	Monocrystalline solar 6 inches
Number of cells	60

Table 1. PV modules characteristics (Nicolaides & Associates, 2019)

ii. Inverter

The PV Modules produce D.C. electric power. This power is converted to A.C. electric power with the use of an inverter. The system also utilizes a Maximum Power Point Tracker-MPPT which constantly regulates the output of the PV panel so as to match the battery or grid.

iii. Support Structure

The support structure is of the fixed type poles. They are made of galvanized steel and they are directly fixed to the ground in cement fixtures. Figure 21 below shows the dimensions and inclination angle of the structure and PV panels.

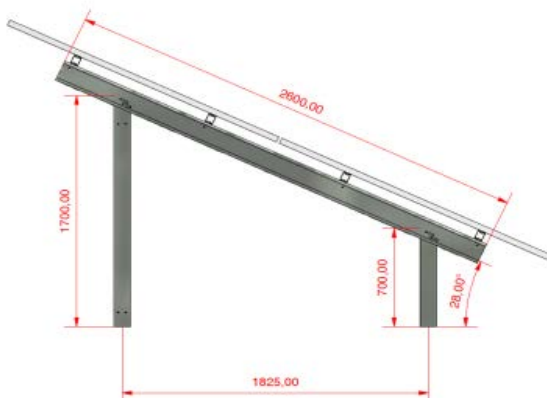


Figure 21. Dimensions and Inclination Angle of the Structure and PV Panels (Nicolaides & Associates, 2019)

4.2.4 Glint and Glare Phenomenon from PV panels

It has already been discussed in paragraph 2.2 that glint and glare is possible under certain conditions. The PV modules of the specific project have anti-glaring glass in order to minimize glint and glare. In addition, glint and glare from PV modules is compared to other surfaces and materials present in the area in order to demonstrate whether or not the PV farm will have a negative glare contribution to the Airport and the environment in general. Figure 22 below indicates that PV solar panels have much less solar reflection than other common surfaces which are present in the area such as soil and concrete.

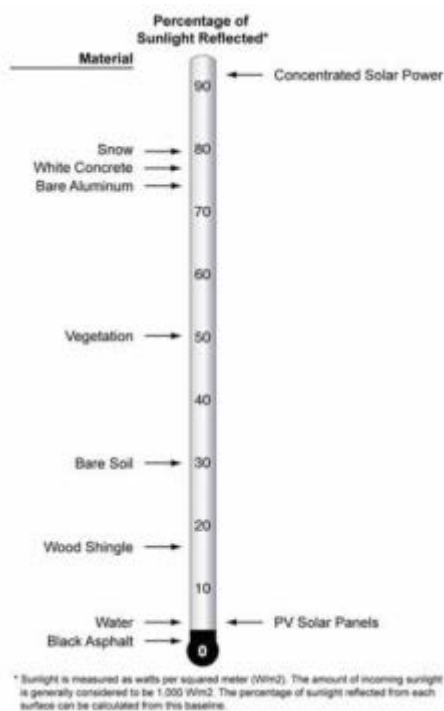


Figure 22. Reflectivity of PV Modules and Other Material (ForgeSolar, 2019)

The results indicated in figure above are also demonstrated in the following table which shows the reflectiveness of several materials with regards to different incident angles.

Surface	Approximate Percentage of Light Reflected ²⁸
Snow	80
White Concrete	77
Bare Aluminium	74
Vegetation	50
Bare Soil	30
Wood Shingle	17
Water	5
Solar Panels	5
Black Asphalt	2

Table 2. Relative reflectivity of different materials (PagerPower, 2019)

From table 2 it is evident that PV panels have much lower reflectiveness than other common materials.

4.2.3 Glint and Glare Assessment

Among the licensing requirements of the PV farm, is the submission of a glint and glare assessment. The assessment should demonstrate that the PV panels do not reflect solar radiation in any manner which might pose danger to any of the following situations:

- Reflection affecting the air traffic control tower
- Low potential for after-image during the final approach (landing) or take off

According to the FAA Technical Guidance which is adopted by the Cyprus Civil Aviation Authority as did most other National Authorities worldwide, the glare assessment should take into consideration an area of 3.2km radius around the landing lanes.

The glare assessment uses GlareGauge, the software developed by FAA for glare assessment purposes. The initial software developed was under the name SGHAT and it was available to all interested users but nowadays it is only available and used by U.S. government and military purposes.

The input parameters used in the software are outlined below.

a. PV Farm Geographical Location

The PV farm was divided in two parts, PV array 1 και PV array due to the arrangement of the PV modules. The time zone used for Cyprus was UTC/GMT +2 hours. The two arrays are shown in figure 23 below.



Figure 23. Larnaca Airport PV Panels Arrays(Nicolaidis & Associates, 2019)

b. Flight Paths

The landing and take-off patterns were chosen based on data and relevant maps available with the Cyprus Civil Aviation Department. Two different flight paths were studied. These flight paths are shown in Figure 25.

c. Analysis Parameters

The parameters which are needed for the software analysis are the following:

i. Units Height (m): The PV modules height of the ground and the height of the observation points at all times.

ii. Time interval: This is the frequency per which the data will be collected. The position of the sun is calculated for the requested time period. For this assessment, the time interval was set at 1 minute and the time period to 12 months.

iii. Subtended angle of the sun: This is the angle defined by the perimeter of the sun as it is perceived by an observer on earth as it is shown in figure 24 below. This is calculated to be 32 degrees or 9,3 mrad ή 0,5°.

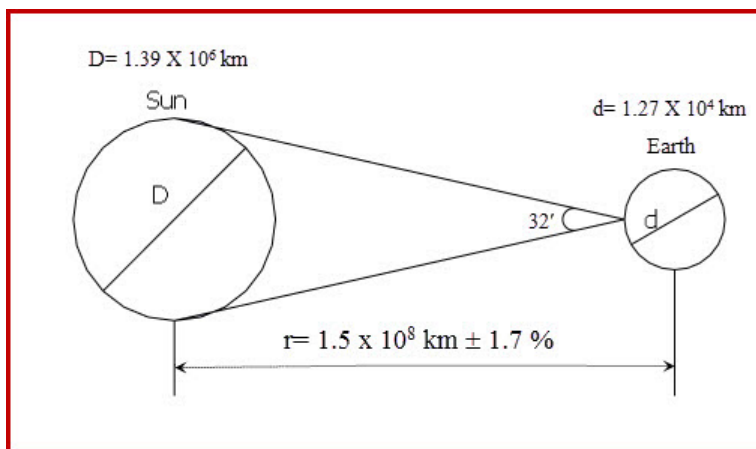


Figure 24. Subtended angle of the sun (Ecoursesonline, 2021)

iv. Direct Normal Irradiation (DNI)(W/m²) : This is the maximum direct normal irradiation which can be observed at a certain geographical location. This value can escalate at any given time in relation to the position of the sun throughout the day. In a typical clear sunny day, a typical value for DNI would be around to 1000 W/m². For the area under study, the maximum DNI on a clear day was calculated to be 1040 W/m².

v. Ocular transmission coefficient: This is the amount of radiation absorbed by the eye before it reaches the retina (see Figure 2). The typical value is 0.5.

vi. Pupil diameter: Pupil is the black circle of the eye and its function is to allow light to reach the retina. Typical values range from 0,002m during the day and 0.008m during night.

vii. Eye focal length: This is the distance between the point where the light rays cross inside the eye and where they intersect the retina (distance f in figure 2). This value is useful in order to calculate the size of the projected image on the retina for a given angle. A typical value is 0,017 m.

viii. Axis Tracking: Defines whether or not axis tracking is employed with values being none/single/dual based on the description given in Paragraph 3.2.3-Tracking Systems. In this particular project, the Axis Tracking is "None".

ix. Panel tilt: PV module tilt is 28°

x. Orientation: The orientation of the arrays is south (180° from true North, as explained in Paragraph 3.2).

xi. Rated power: The PV farm rated power is 3500kW.

xii. Module surface material: The modules' material is anti-reflective deeply textured glass.

xiii. Reflectivity varies with incidence angle: If this parameter is selected, the software calculates the reflectivity of the PV modules in relation of the sun's position at every time interval. For this assessment, the value 0.2 was selected.

ixx. Correlate slope error to module surface type: If this parameter is selected, the software calculates the slope error in relation to the PV surface material. For the assessment the parameter was selected and the slope error was calculated to be 83mrad.

xx. Height above ground: This is the PV modules height above ground and for this project it was 1,47m

xxi. Flight Path:

xxii. Direction: Direction from the lower point (threshold) along which observation point are defined (0° = north, 90° = east of north) Direction for Flight Plan FP1 is 41° και for Flight Path FP 2 is 221° .

xxiii. Glide slope: This is the angle of descent or ascent during landing and take-off respectively. For this project this was 3° for FP1 and 2.75° for FP2.

xxiv. Threshold crossing height: This is the height of the plane when crossing the lowest point (threshold). For this assessment this was 15.24m.

xxv. Consider pilot visibility from cockpit: If this parameter is selected, the user can define the limits of the viewing angles of the pilot through the cockpit. If not selected, the software uses typical parameters as follows:

- Maximum descent viewing angle: 30 °
- Azimuth viewing angle: 120 °

For the assessment, this parameter was not selected as the typical values were considered satisfactory.

The following figure indicates the PV array locations, the Air traffic Control Tower and the Flight Paths.



Figure 25. PV array locations, Airtraffic Control Tower and Flight Paths(Nicolaides & Associates, 2019)

4.2.4 Assessment Results and Conclusions

The assessment results are shown in figure 26 below. For the calculations a time interval of 1minute was considered. Detailed presentation of the results is shown in Appendix 1.

a. Assessment results

According to the results in Appendix 1 there is not any glare effect on the Air Traffic Control Tower or on Flight Path 2, from either of the two arrays.

On Flight Path 1 there is a possibility of glare effect for 27091 minutes per year during the hours between 06:00am and 10:00am of the same day. According to FAA guidelines this is considered acceptable.

b. Conclusions

Based on the assessment results above, the location and other parameters (inclination, orientation) of the PV arrays, have only “Low Potential for After Image” (see figure 3), which is considered acceptable according to the “Technical Guidance for Evaluating Selected Solar Technologies on Airports” of FAA.

Furthermore, the anti-reflective deeply textured glass of the PV modules prevents unwanted radiation from reaching the observation points. The surface of sea water and the dried up in the summer salt lake, have greater glare effect than PV modules.

Chapter 5

Proposed Project Assessment

The proposed project is the deployment of a PV farm within the surrounding area of Nicosia General Hospital. The PV farm will be very beneficial to the energy consumption sustainability of the Hospital. The electricity consumption expense of Nicosia General Hospital, is around to 4 million euro per year.

Apart from the financial burden, an organization whose main purpose is to provide health services, needs to be at the forefront of the protection of the environment as well. For the above reasons, it was deemed necessary to introduce measures for reducing energy consumption, and the deployment of a PV farm is one of the main actions towards a more sustainable, environmentally friendly operation.

This assessment is of great importance due to the close proximity of the PV farm to the Hospital's Helipad (250m approximately). Should there be any danger to helicopter flights from glare, not only the helicopter personnel and passengers but also the Hospital's patients, personnel and the Hospital's operations will be jeopardized.

5.1 Assessment Methodology

In order to carry out a thorough glare assessment, the following methodology is followed:

- a. Identify the location of the proposed project. The area under examination is defined at a radius of 3.2m (see paragraph 4.2.3 -Glint and Glare Assessment).
- b. Specify the receptor points to be considered for glare effect. For the proposed installation, these points are inside the helicopter cockpit along the flight paths. At the Hospital's location there is not an Air Traffic Control Tower.
- c. Execute GlareGauge software tool with appropriate inputs.

- d. Evaluate software tool results and identify glare issues.
- e. Suggest improvements and or alternative solutions in order to eliminate glare issues.
- f. Execute GlareGauge software tool with alternative inputs and reassess the results.

5.2 Nicosia General Hospital Description

The Hospital is the largest medical facility in the Country. It is the most equipped Hospital as far as medical equipment is concerned and it has the highest yearly patient treatment visitation figures. More than 25,000 patients are hospitalized for treatment, over 250,000 patients are admitted to outpatient care facilities, more than 100,000 patients visit the Accidents and Emergency Department and around to 7,500 surgeries are performed each year. Nicosia General Hospital is the only medical facility in Cyprus providing tertiary care. It is considered to be the country's reference Hospital.

In the Hospital, 2300 people are employed from different professions, such as doctors, nurses, laboratory employees, technicians, workers and administration staff. It is also estimated that more than 2500 people, other than employees, visit the Hospital every day (patients, visitors, patients' relatives, Hospital associates).

The Hospital comprises of over 100,000 square meters of covered spaces. It is a 6 floor level structure with medical facilities in Levels -1,0,1,2,3 and 4. There are 24 different Wards/Clinics, Outpatient Department, Radiology Department, Clinical Laboratories, Accidents and Emergency Department, Surgery Department, Blood Bank, Morgue, Kitchen, Laundry Facility, Warehouse and Administration Department.

5.3 Facilities Location

The Site where the PV farm will be deployed is Nicosia General Hospital. The Hospital is situated at the South outskirts of Nicosia, as shown within a red perimeter line in an aerial plan view (Google Maps, 2021), in Figure 26 below.



Figure 26. Nicosia General Hospital (Google Maps, 2021)

5.4 Description of PV Project

The proposed installation involves a PV farm of 943kW capacity. The PV farm will be supplying power to the Hospital. It is not expected that there will be any surplus power to be diverted to the Cyprus Electric Authority power grid.

5.4.1 PV Farm Location

The proposed project consists of two PV arrays as shown in Figure 27 below in red perimeters. A more detailed plan view of the PV Arrays is shown in Appendix 2.

The Helipad is shown within a blue perimeter and the Hospital's Main Buildings are shown within a green perimeter.



Figure 27. Proposed PV Farm Location (Google Maps, 2021)

5.4.2 Nicosia General Hospital PV Farm Technical Characteristics

Following are the PV farm technical characteristics, such as capacity and PV modules technical specifications.

a. PV Modules

The proposed PV farm capacity is as follows:

i. PV Array 1

Quantity of Photovoltaic Modules	1749
Capacity per Module	400w
Total Array 1 Capacity	700kW

ii. PV Array 2

Quantity of Photovoltaic Modules	608
Capacity per Module	400w
Total Array 2 Capacity	243kW

$$\text{Total PV Farm Capacity} = \text{Array 1 Capacity} + \text{Array 2 Capacity} = 943\text{kW}$$

The installed PV capacity is calculated by considering the footage area of the PV module based on its dimensions as depicted by the datasheet of PERC SOLAR CELL in Appendix 3:

Panel height 2.008m

Panel width 0.992m

Installation angle 33°

Area footage per panel = $2.008\text{m} \times \cos 33^\circ \times 1.002\text{m} = 1.69\text{m}^2$

Capacity 400W

c. Support Structure

The PV modules will be installed on a fixed structure without rotational capability. The structure will be raised to 2.5m height at its lower point so it can be used over the parking space for shading purposes as well.

5.4.3 Cost Benefit Analysis for PV System installation

From market research, the investment in PV system supply and installation will be around to 900Eur per installed kW. So, for the proposed 943kW system, the cost will be approximately 850,000Eur. Additionally, there will be a further cost of 500,000 euro for the support structure over the parking lot, for a total investment cost of 1,350,000 Eur.

The solar capacity in Cyprus is estimated at 1700kWh per installed kW (George Makrides, Bastian Zinsser, Matthew Norton, George E. Georghiou, Markus Schubert and Jürgen H. Werner, 2008). Thus the capacity of the proposed system will be $943\text{kW} \times 1700\text{kWh/kW} = 1,603 \text{ MWh/year}$

Based on the tariff of 0.17 Eur/kWh, the economic benefit is $1,603,000 \times 0.17 = 272,510$ Eur/year. Thus, the investment payback period can be calculated as $1,350,000 / 272,500 = 5$ years.

Should one consider only the photovoltaic modules' cost and not the carpark shade advantage, the investment payback period would be $850,000 / 272,500 = 3.1$ years

From above investment payback period, the investment is considered economically viable.

5.4.4 Glint and Glare Assessment

Following are the data and assumptions used for the glare assessment of the proposed installation.

a. PV Farm Geographical Location

The Hospital's parking lot is divided in two main sections. The proposed PV arrays will be installed over each one of this two sections as shown in figure 27. From the European Commission's PHOTOVOLTAIC GEOGRAPHICAL INFORMATION SYSTEM website (Appendix 2), the geographical coordinates of the site are 35.127, 33.376 (Latitude, Longitude). The time zone used for Cyprus was UTC/GMT +2 hours.

b. Flight Paths

The Cyprus Civil Aviation Department provided with the map of Appendix 6. The map indicates the area of approach and take off to the Helipad. The map indicates in red triangles the areas which are avoided by the helicopters. Three different, two way flight paths were studied, covering the area within the red areas. These flight paths are shown in Figure 28. The receptor points are considered to be inside the cockpit along the flight paths at a radius of 3.2km from the PV Arrays.

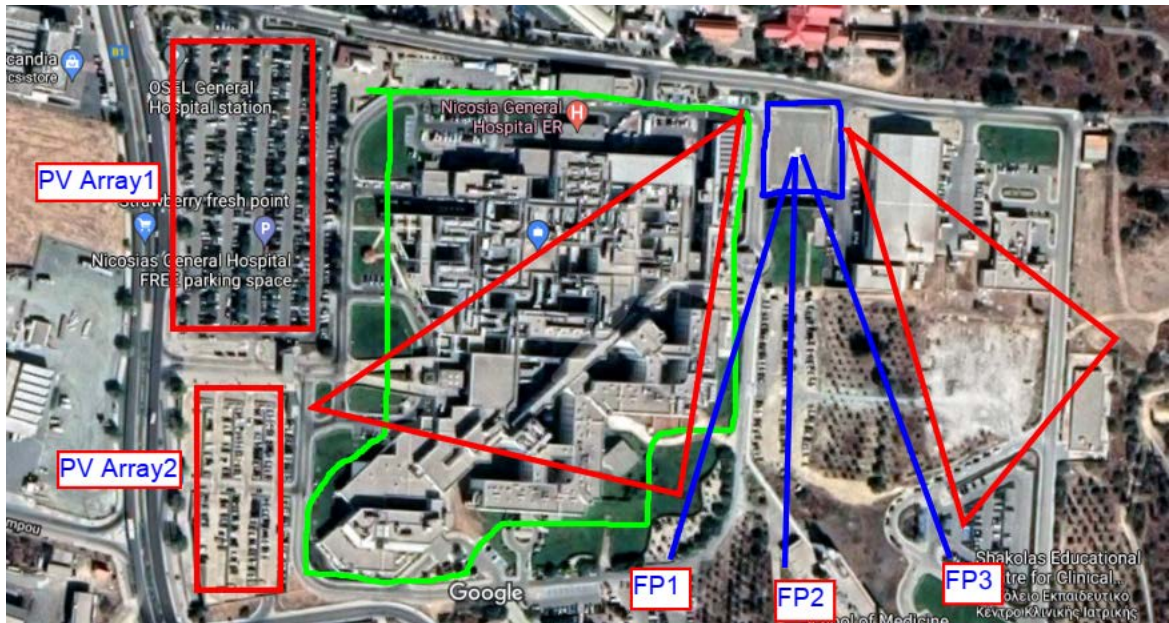


Figure 28. Helicopter Flight Paths (Cyprus Civil Aviation Department)

d. Analysis Parameters

The parameters which are needed for the software analysis are the following:

i. Units Height (m): The PV modules height of the ground and the height of the observation points at all times.

ii. Time interval: This is the frequency per which the data will be collected. The position of the sun is calculated for the requested time period. For this assessment, the time interval was set at 10 minutes (minimum time interval allowed for GlareGauge software demo mode) and the time period to 12 months.

iii. Subtended angle of the sun: This is the angle as it was shown in figure 24. This is calculated to be 32 degrees or 9,3 mrad ή 0,5°.

iv. Direct Normal Irradiation (DNI)(W/m²) : This is the maximum direct normal irradiation which can be observed at the geographical location of Nicosia General Hospital. From the European Commission's PHOTOVOLTAIC GEOGRAPHICAL INFORMATION SYSTEM website (Appendix 4), for the specific project location,

this was calculated for the months of June, July and August. The maximum value was found to be 800 W/m^2 in the month of August. For the glare assessment, the default value of 1000 W/m^2 was used as the worst case scenario.

v. Ocular transmission coefficient: The typical value is used of 0.5.

vi. Pupil diameter: The typical values were used ranging from 0,002m during the day and 0.008m during night.

vii. Eye focal length: A typical value is used of 0,017 m.

viii. Axis Tracking: Axis tracking is not thus the value Axis Tracking "None" is selected.

ix. Panel tilt: PV module tilt is 33° , based on the geographical longitude.

x. Orientation: The orientation of the arrays is south (180° from true North, as explained in Paragraph 3.2).

xi. Rated power: The PV farm rated power is 943kW.

xii. Module surface material: The modules' material is anti-reflective deeply textured glass.

xiii. Reflectivity varies with incidence angle: For this assessment, the value 0.2 was selected.

ixx. Correlate slope error to module surface type: This parameter was selected, so that the software calculates the slope error in relation to the PV surface material.

xx. Height above ground: This is the PV modules height above ground and for this installation it is calculated as follows:

$$\text{length} \times \sin 33^\circ + 2.5\text{m} = 2,008\text{m} \times \sin 33^\circ + 2.5\text{m} = 3.6\text{m}$$

xxi. Flight Path: 3 different two way flight paths as shown in figure 28

xxii. Direction: Direction from the lower point (threshold) along which observation point are defined (0° = north, 90° = east of north). Direction for both flight paths is 90° .

xxiii. Glide slope: This is the angle of descent or ascent during landing and take-off respectively. For this project this was 3° for all flight paths.

xxiv. Threshold crossing height: This is the height of the plane when crossing the lowest point (threshold). For this assessment this was considered to be the height of the Hospital (15m) since below that it is not possible to have direct viewing of the PV modules from the helicopter's cockpit.

xxv. Consider pilot visibility from cockpit: If this parameter is selected, the user can define the limits of the viewing angles of the pilot through the cockpit. If not selected, the software uses typical parameters as follows:

- Maximum descent viewing angle: 30 °
- Azimuth viewing angle: 120 °

For the assessment, this parameter was not selected as the typical values were considered satisfactory.

5.5. Presentation of results and discussion

The data presented in paragraph 5.4.4 are inserted in GlareGauge software. The analysis is carried out for all three Flight Paths (FP1, FP2 and FP3), for each Photovoltaic Array separately (PV1 and PV2) for a total of six times. The results of the six assessments are presented in Appendix 5.

Due to the location of the Helipad, Hospital Management Team set the requirement of no glare with potential to cause an after-image (flash blindness).

5.5.1 Assumptions and Simplifications

The assessment was carried out using the following assumptions and simplifications:

- i. "Green" glare is denoted as glare which has low potential to cause an after-image (flash blindness).
- ii. "Yellow" glare is denoted as glare which has potential to cause an after-image (flash blindness).
- iii. GlareGauge software does not account for any obstacles between the PV arrays and the view from the Flight Paths.
- iv. There is always clear sky without cloud shading over the PV arrays.
- v. The PV modules are always clean and clear from debris and dust.
- vi. The incident radiation angle from all PV modules of the same PV Array, is the same.
- vii. The reflected radiation angle from all PV modules of the same PV Array, is the same.

These assumptions and simplifications, all account for the “worst case scenario”. If the assessment results do not indicate any possible danger from glare for the particular

Helipad, then there is a greater margin of safety than the one built into the GlareGauge Software.

5.5.2 Assessment Results

The summary results from the simulations in Appendix 5 are shown in Table 3 below.

PV Array	Flight Path	Simulation Results – Possibility of “green” glare in minutes per year	Simulation Results – Possibility of “yellow” glare in minutes per year
PV1	FP1	0	0
PV1	FP2	0	0
PV1	FP3	152	365
PV2	FP1	0	0
PV2	FP2	0	0
PV2	FP3	391	0

Table 3. Simulation Results

From above table, four of the six flight path assessments do not show any glare from either of the two PV arrays. Assessment for Flight path FP3 shows 152 minutes of “green” glare and 365 minutes of “yellow” glare from Photovoltaic Array PV1, over a period of 12 months. Also, the assessment for same Flight Path FP3 shows 391 minutes of “green” glare from Photovoltaic Array PV2, over a period of 12 months.

As explained in Paragraph 2.2.1, “green” glare has low potential for afterimage and “yellow” glare has potential for afterimage.

While no mitigation measures are required for the “green” glare produced, the requirement set at the beginning of the current paragraph for “yellow” glare being not acceptable, calls for mitigation measures.

5.5.3 Maximum Annual Energy Production

One of the goals of the Thesis is to calculate the maximum annual energy production of the PV Arrays in order to verify the economic viability of the system. Another feature of the GlareGauge software is the prediction of the annual energy production.

From Appendix 5, the predicted annual energy production per PV Array is as follows:

PV Array 1	1,681,000.00kWh
<u>PV Array 2</u>	<u>583,200.00kWh</u>
TOTAL	2,264,200.00kWh

This prediction is much higher than the annual production of 1,603,000.00kWh estimated in paragraph 5.4.3.

According to the GlareGauge prediction, the investment payback period can be calculated as follows:

$$\text{a) } \frac{\text{Investment Cost (with car park shading)}}{\text{(Total Annual Production x Electricity Tariff)}} = \frac{1,350,000}{2,264,200 \times 0.17} = 3.5 \text{ years}$$

$$\text{b) } \frac{\text{Investment Cost (without car park shading)}}{\text{(Total Annual Production x Electricity Tariff)}} = \frac{850,000}{2,264,200 \times 0.17} = 2.2 \text{ years}$$

Based on the above calculations, the payback period is even better than what was initially anticipated.

5.5.4 Mitigation Measures

Due to the requirement of eliminating the possibility of “yellow” glare, the software simulation was run again using a different PV module material. This time instead of PV modules with Smooth Glass with Anti Reflective Coating, Deeply Textured Glass PV modules were assumed for the Photovoltaic Array 1.

The simulation results are shown in Appendix 5 (Flight Path 3 (PV Array 1) GlareGauge Assessment – Mitigation Assessment). From these results it is now evident that “yellow” glare is eliminated. The only glare present is “green” glare for 4663 minutes per year which is acceptable since it has only low potential for afterimage.

5.5.5 Conclusions

As stated in the Summary Section, the Thesis attempts to investigate the global concern on the effect of glint and glare from Photovoltaic (PV) farms on aviation travel, the attempts made to regulate their development in different countries, strengthen or contradict the global perception of glare risks and asses the effect of a PV farm in close vicinity to Nicosia General Hospital’s Helipad.

From the Thesis it is evident that there is great concern regarding glare from photovoltaic farms when these are close to Airports and other aviation landing places such as Helipads. In the Thesis further investigation was carried out and the regulation attempts in different countries are presented.

The large number of PV farm installations already in place for Airport electricity demand supply shows the need for and the importance of this technology. In addition to the installations presented in Chapter 4, the Solar Trade Associations (STA) report, which is considered to be the most up-to-date compilation of analysis relating to glint and glare and their effect on aviation travel, has examined *“Over 200 glint and glare assessments conducted for airports and developers”*. Out of these 200 assessments, 80% did not indicate any glare issues, 17,5% needed to be investigated further but again did not indicate any glare issues and only for 2.5% of the assessments regarding 5 cases, the original design had to be revised before approval has been given.

The particular assessment for Nicosia General Hospital’s Helipad, falls within the above 2.5%. Due to the requirement for not any glare even with potential for after image (“yellow” glare), the original PV module material was changed. Instead of the original Smooth Glass with Anti Reflective Coating modules, Deeply Textured Glass PV modules were used for the Photovoltaic Array 1. This design change eliminated the potential for after image (“yellow” glare) which was downgraded to “low” potential for after image (“green” glare). This stresses the importance of the Thesis and of the glare assessments which assist in eliminating danger which would not have been otherwise realized.

In addition to the safeguarding of the Helicopter flights and all related people and assets concerned, the assessment in the Thesis proved that the investment is profitable and actually it is even better than the original estimate. This is an important factor since now the project is well documented not only with regards to safety but also with regards to its’ economic sustainability.

References

1. Air Transport Action Group, 2020, "Power from the sun", Available at: <https://aviationbenefits.org/case-studies/power-from-the-sun/>, [Accessed 4th November, 2020]
2. Nicola Pearsall, 2016, "The Performance of Photovoltaic (PV) Systems", Available at: <https://learning.oreilly.com/library/view/the-performance-of/9781782423546/> [Accessed 10th October, 2020]
3. U.S Department of Transportation (Federal Aviation Administration, FAA), 2018, "Technical Guidance for Evaluating Selected Solar Technologies on Airports", Available at: https://www.faa.gov/airports/environmental/policy_guidance/media/FAA-Airport-Solar-Guide-2018.pdf, [Accessed 10 December, 2020]
4. U.S Department of Transportation(Federal Aviation Administration, FAA), , 2019, "ORDER JO 7400.2M - Procedures for Handling Airspace Matters", Available at: <https://www.faa.gov/documentLibrary/media/Order/7400.2M Bsc w Chg 1 dtd 1-30-20.pdf>, [Accessed 10 November, 2020]
5. U.S. Department of Transportation (Federal Aviation Administration, FAA), 2013, "Interim Policy 78 FR 63276, FAA Review of Solar Energy System Projects on Federally Obligated Airports", Available at <https://www.govinfo.gov/content/pkg/FR-2013-10-23/pdf/2013-24729.pdf>, [Accessed on 10 October, 2020]
6. 'Aviation Benefits Beyond Borders'
7. World's Resources Institute, 2016, "Bangalore's Airport to Become a Leader in Solar Energy Production", Available at: <https://www.wri.org/blog/2016/09/bangalores-airport-become-leader-solar-energy-production>, [Accessed April 3rd, 2021]
8. James Momoh, 2018, "Energy Processing and Smart Grid", Available at: <https://onlinelibrary.wiley.com/doi/book/10.1002/9781119521129>, [Accessed 22 October, 2020]
9. Ho, C. K., Ghanbari, C. M., and Diver, R. B., 2009, "Hazard Analyses of Glint and Glare From Concentrating Solar Power Plants", Available at: https://share-ng.sandia.gov/glare-tools/references/Glint_Glare_SolarPACES2009.pdf [Accessed 3rd December, 2020]
10. Forgesolar, 2019, "Guidance and information on using ForgeSolar analysis tools", Available at: <https://www.forgesolar.com/help/>, [Accessed 10 October, 2020]
11. Yellowhair, J. and C.K. Ho. , 2015, "Assessment of Photovoltaic Surface Texturing on Transmittance Effects and Glint/Glare Impacts", Available at:

- <https://www.forgesolar.com/static/docs/yellowhair-2015-asmt-pv-surf.pdf>
[Accessed 2nd November, 2020]
12. Balkan Green Energy News, 2020, "Solar power project in Cyprus continues after delay to protect orchids", Available at: <https://balkangreenenergynews.com/solar-power-project-in-cyprus-continues-after-delay-to-protect-orchids/> [Accessed 13 October, 2020]
 13. CAA INTERIM GUIDANCE
<https://unidoc.wiltshire.gov.uk/UniDoc/Document/File/MTMvMDUyNDQvRIVMLDQ2MTEwNg==>
 14. Leitlinie des Ministeriums für Umwelt (Federal Ministry of the Environment), 2014, "Gesundheit und Verbraucherschutz zur Messung und Beurteilung von Lichtimmissionen (LichtLeitlinie)", Available at: http://www.mlul.brandenburg.de/media_fast/4055/licht_leitlinie.pdf, [Accessed 12 February, 2021]
 15. Gevorkian Peter, 2008, "Solar Power in Building Design, 1st edition." United States of America: McGraw-Hill, 2008
 16. Sustainable Energy Authority of Ireland (SEAI), 2016, "Planning and Development Guidance Recommendations for Utility Scale Solar Photovoltaic Schemes" Available at: https://www.seai.ie/publications/2016_RDD_96_Planning_Development_Guidance_Utility_Solar_PV_Irl_-_FAC.pdf, [Accessed 9 February, 2021]
 17. M.M. Fouada, Lamia A. Shihatab, ElSayed I. Morgan, 2017, "An integrated review of factors influencing the performance of photovoltaic panels", Available at: <https://www.sciencedirect.com/science/article/abs/pii/S1364032117307803>
[Accessed 14 March, 2021]
 18. U.S Department of Energy, 2021, "Solar Photovoltaic Technology Basics", Available at: <https://www.energy.gov/eere/solar/solar-photovoltaic-technology-basics>, [Accessed 2nd April, 2021]
 19. Innovision, 2019, "Solar Photovoltaic Glint & Glare Study Aviation Specific (Dublin Airport)", Available at: <https://www.pleanala.ie/publicaccess/EIAR-NIS/305623/Planning%20Application%20Reports/Other/Glint%20and%20Glare%20Study.pdf>, [Accessed 25 January, 2021]
 20. Stephen Peake, 2018, "Renewable Energy: Power for a Sustainable Future, 4th ed. " Oxford, UK: Oxford University Press

21. University of Calgary, Energy Education, 2018, “ *Types of photovoltaic cells*”, Available at: https://energyeducation.ca/encyclopedia/Types_of_photovoltaic_cells, [Accessed 12 March, 2021]
22. John R. Balfour, 2011, “Introduction to Photovoltaic System Design”, Available at: <https://www.oreilly.com/library/view/introduction-to-photovoltaic/9781449624675/> [Accessed 11 March, 2021]
23. John R. Balfour, 2011, “*Advanced Photovoltaic Installations*”, Available at: <https://www.oreilly.com/library/view/advanced-photovoltaic-installations/9781449624712/> [Accessed 12 March, 2021]
24. Kaddoura, Tarek & Anwari, Makbul & Al-Turki, Yusuf. ,2016, “*On the estimation of the optimum tilt angle of PV panel in Saudi Arabia. The Open Renewable Energy Journal*”. Available at: https://www.researchgate.net/publication/305506106_On_the_estimation_of_the_optimum_tilt_angle_of_PV_panel_in_Saudi_Arabia [Accessed 18 March, 2021]
25. PagerPower, 2019, “ *Solar Photovoltaic Glint and Glare Study*”, Available at: <https://cleaneartenergy.com/wp-content/uploads/2020/03/Pines-Tip-Glint-and-Glare-Assessment.pdf> , [Accessed 23 March, 2021]
26. Ecoursesonline website, 2021, “ *Lecture 11 Solar Radiation* ” Available at: <http://ecoursesonline.iasri.res.in/mod/page/view.php?id=1625>, [Accessed 10 April, 2021]
27. Solar Trade Associations (STA) (2016), “ *Impact of solar PV on aviation and airports*”, Available at: <http://www.solar-trade.org.uk/wp-content/uploads/2016/04/STA-glint-and-glare-briefing-April-2016-v3.pdf>, [Accessed 22 April, 2021]
28. Prologis (2021), “ Prologis Park Narita 1-A, B”, Available at: <https://www.prologis.com/industrial-logistics-warehouse-space/japan/narita/prologis-park-narita-1-b>, [Accessed 10 October, 2020]
29. Airport Experience News (2020), “ *PIT BEGINS CONSTRUCTION OF NEW MICROGRID*”, Available at: <https://airportxnews.com/pit-begins-construction-new-microgrid/>, [Accessed 10 October, 2020]
30. C&S Engineers, Inc. (2012), “ *Fresno Yosemite Airport Sustainability Management-Plan*”, Available at: <https://www.faa.gov/airports/environmental/sustainability/media/Fresno->

- [Yosemite-Airport-Sustainability-Management-Plan.pdf](#), [Accessed 15 October, 2020]
31. Greenaironline (2012), “Athens International begins operation of the world's largest airport photovoltaic installation”, Available at: <https://www.greenaironline.com/news.php?viewStory=1350>, [Accessed 16 October, 2020]
 32. Munich Airport (2019), “Sustainability Program 2019”, Available at: https://www.munich-airport.de/_b/0000000000000009259601bb5ef494d6/ib2019-sustainability-program.pdf, [Accessed 18 October, 2020]
 33. WSP Global Inc. (2021), “Renewable Energy at Madrid, Barcelona, Tenerife and Mallorca Airports”, Available at: <https://www.wsp.com/en-TH/projects/renewable-energy-at-madrid-barcelona-tenerife-and-mallorca-airports>, [Accessed 18 April, 2021]
 34. Nicolaidis & Associates (2019), “ΜΕΛΕΤΗ ΑΝΤΑΝΑΚΛΑΣΗΣ ΑΠΟ ΤΗΝ ΛΕΙΤΟΥΡΓΙΑ ΜΟΝΑΔΑΣ ΠΑΡΑΓΩΓΗΣ ΗΛΕΚΤΡΙΚΗΣ ΕΝΕΡΓΕΙΑΣ ΜΕ ΦΩΤΟΒΟΛΤΑΪΚΟ ΣΥΣΤΗΜΑ ΣΥΝΟΛΙΚΗΣ ΙΣΧΥΟΣ 3.5MW ΣΤΟ ΑΕΡΟΔΡΟΜΙΟ ΛΑΡΝΑΚΑΣ ΤΗΣ ΕΤΑΙΡΕΙΑΣ ERMES AIRPORTS LTD (ΑΝΑΘΕΩΡΗΜΕΝΗ)”, Available at: [http://www.moa.gov.cy/moa/environment/environmentnew.nsf/All/B1C2AC287753464DC225837C0023D471/\\$file/ES20190020102.pdf?OpenElement](http://www.moa.gov.cy/moa/environment/environmentnew.nsf/All/B1C2AC287753464DC225837C0023D471/$file/ES20190020102.pdf?OpenElement), [Accessed 18 March, 2021]
 35. European Commission, 2021, “PHOTOVOLTAIC GEOGRAPHICAL INFORMATION SYSTEM”, Available at: https://re.jrc.ec.europa.eu/pvg_tools/en/tools.html, [Accessed 29 April, 2021]
 36. George Makrides, Bastian Zinsser, Matthew Norton, George E. Georghiou, Markus Schubert and Jürgen H. Werner (2008), “Energy Yield of Different Photovoltaic Systems Installed in Cyprus”, Available at: https://www.researchgate.net/publication/238066898_Energy_Yield_of_Different_Photovoltaic_Systems_Installed_in_Cyprus, [Accessed 5 January, 2021]

Appendix 1. Larnaca Airport Glare Analysis Results

GLARE ANALYSIS RESULTS

Summary of Glare

PV Array Name	Tilt (°)	Orient (°)	"Green" Glare min	"Yellow" Glare min	Energy kWh
PV array 1	28.0	180.0	14,548	0	-
PV array 2	28.0	180.0	12,543	0	-

Total annual glare received by each receptor

Receptor	Annual Green Glare (min)	Annual Yellow Glare (min)
FP 1	27091	0
FP 2	0	0
1-ATCT	0	0

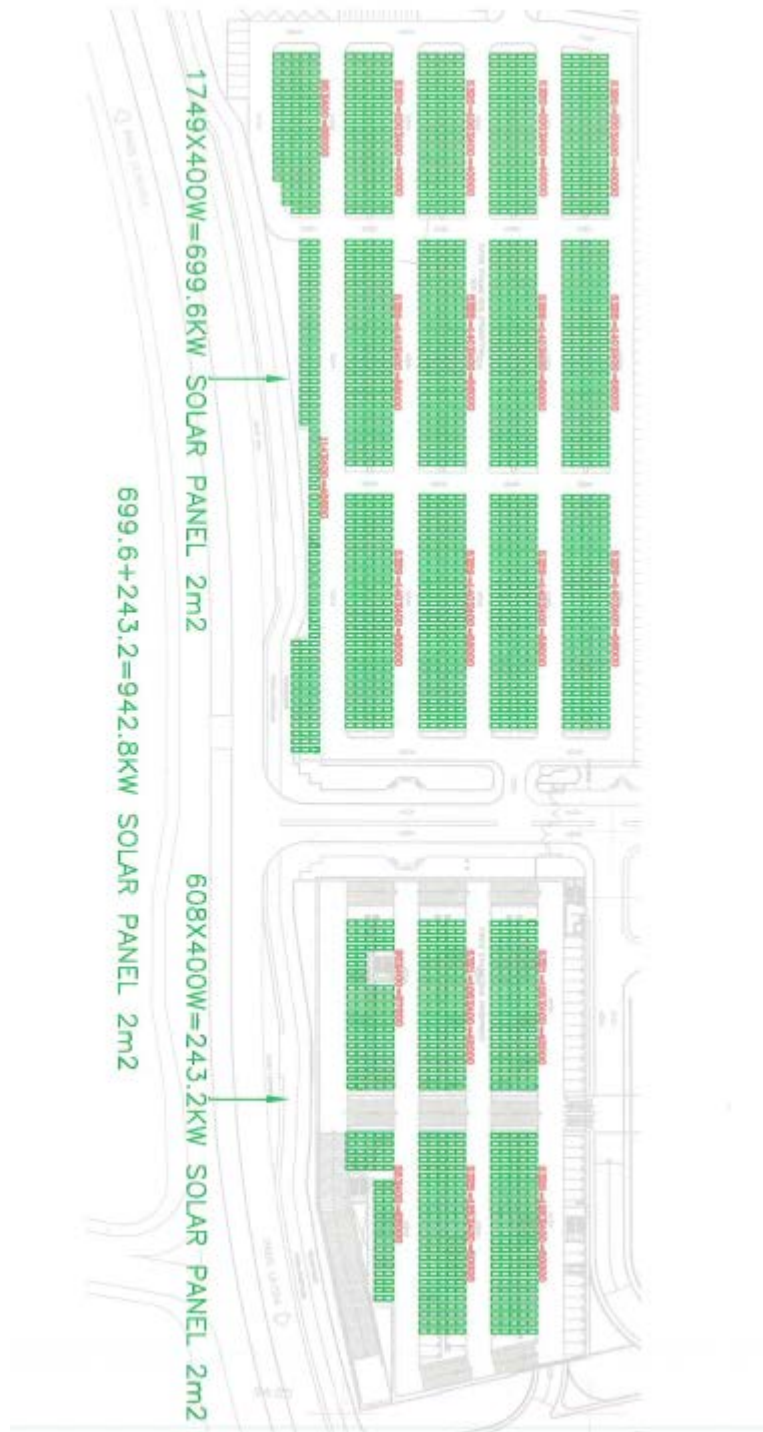
Results for: PV array 1

Receptor	Green Glare (min)	Yellow Glare (min)
FP 1	14548	0
FP 2	0	0
1-ATCT	0	0

Flight Path: FP 1

0 minutes of yellow glare
14548 minutes of green glare

Appendix 2. PV Arrays



Appendix 3. PERC SOLAR CELL PV Panels



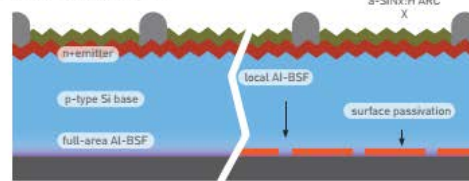
Ultra High Efficiency Solar Module

PERC SOLAR CELL

PERC Solar Cell

- The mono cell technology with Passivated backside and local BSF
- Proprietary Laser Pattern Design Superior AlO_x layer Passivation.

Ag front contacts ("fingers")



Al rear contact

Lower System Cost

Benefit: Save System Costs Per Watt



More Power Per m²

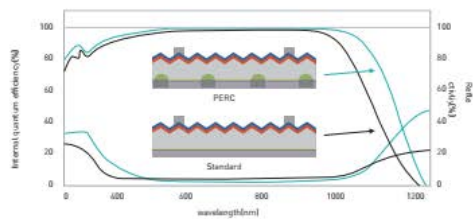
10% more power production per unit area



Benefit: 10% More Power

+10% PERC module 290W VS Standard module 265W

Excellent Low-light Performance




Product Characteristics

Model No.	CSM400-144	CSM410-144
Warranty		
Product Warranty	15 Years	
Power Warranty	12 Years of 92% Output Power, 30 Years of 85% Output Power	
Electrical Data at STC		
Maximum Power (Pmax)	400 Wp	410 Wp
Voltage at Maximum Power (Vmpp)	41.75 V	42.35 V
Current at Maximum Power (Impp)	9.6 A	9.69 A
Open Circuit Voltage (Voc)	49.8 V	50.4 V
Short Circuit Current (Isc)	10.36 A	10.6 A
Panel Efficiency	19.88 %	20.38 %
Power Tolerance (Positive)	+ 5 %	+ 5 %
	<i>Standard Test Conditions (STC): air mass AM 1.5, irradiance 1000W/m², cell temperature 25°C</i>	
Material Data		
Panel Dimension (H/W/D)	2008x1002x40 mm	
Weight	22.5 kg	
Cell Type	Monocrystalline	
Cell Size	158.75x158.75 mm	
Cell Number	144	
Glass Type	Tempered, Anti-reflection Coating	
Glass Thickness	3.2 mm	
Encapsulant Type	EVA	
Back Cover Type	TPT	
Frame Type	Anodized Aluminium Alloy	
Junction Box Diodes	3	
Junction Box Protection Class	IP 68	
Connector Type	MC4	
Cable Crosssection	4 mm ²	
Cable Length	900 mm	

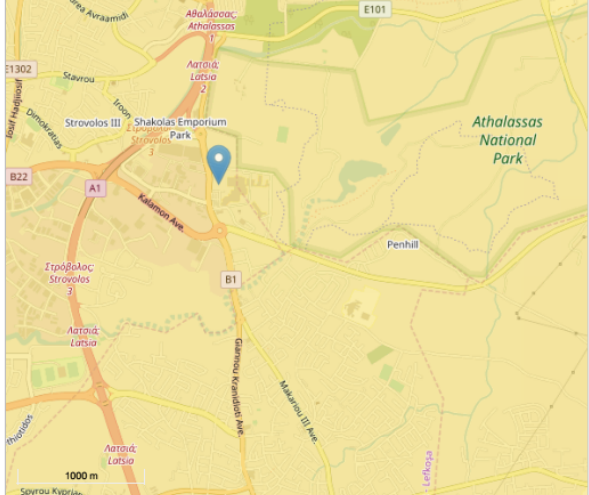
Appendix 4. Photovoltaic Geographical Information

Legal notice | (https://ec.europa.eu/info/legal-notice_en)Cookies | (https://ec.europa.eu/info/cookies_en)Contact | (https://ec.europa.eu/jrc/en/contact/form) English (en)



PHOTOVOLTAIC GEOGRAPHICAL INFORMATION SYSTEM

European Commission (http://ec.europa.eu/index_en.htm) > EU Science Hub (https://ec.europa.eu/jrc/en/) > PVGIS (https://ec.europa.eu/jrc/en/pvgis) > Interactive tools (/pvg_tools/en/tools.html)



Address: Lat/Lon: ()

Cursor:
Selected: 35.127, 33.376
Elevation: 177 (m):

Use terrain shadows:
 Calculated horizon ()
 Upload horizon file ()

No file chosen

AVERAGE DAILY IRRADIANCE DATA

Solar radiation database ()

Month*

UTC time () Local time ()

On fixed plane:
 Irradiance
 Clear-sky irradiance
Slope [°] ()
Azimuth [°] ()

On sun-tracking plane:
 Irradiance
 Clear-sky irradiance

Temperature:
 Daily temperature profile

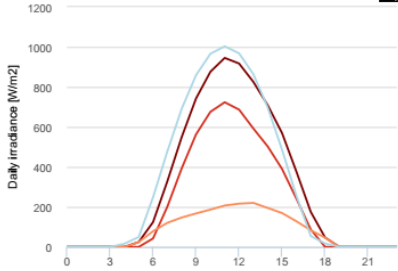
AVERAGE DAILY IRRADIANCE DATA: RESULTS

Fixed-plane Tracking Temperature Info

Summary

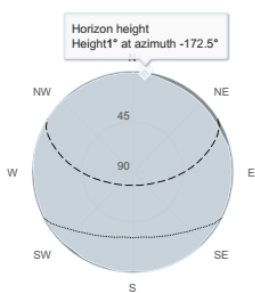
Provided inputs:
Location [Lat/Lon]: 35.127, 33.376
Horizon: Calculated
Database used: PVGIS-SARAH
Month: June

Daily average irradiance



Irradiance (Click on series to hide)
— Global — Direct — Diffuse — Clearsky

Outline of horizon



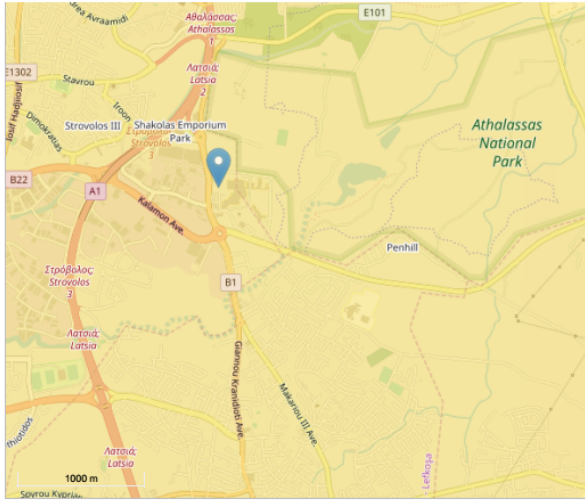
■ Horizon height
-- Sun height, June
--- Sun height, December

Last update: 15/10/2019 [Top](#)



PHOTOVOLTAIC GEOGRAPHICAL INFORMATION SYSTEM

European Commission (http://ec.europa.eu/index_en.htm) > EU Science Hub (https://ec.europa.eu/jrc/en/) > PVGIS (https://ec.europa.eu/jrc/en/pvgis) > Interactive tools (/pvg_tools/en/tools.html)



Cursor:
Selected: 35.127, 33.376
 Elevation: 177 (m)

Use terrain shadows:
 Calculated horizon () [↓ csv](#) [↓ json](#)
 Upload horizon file () [Choose file](#) No file chosen

AVERAGE DAILY IRRADIANCE DATA ⓘ ()

Solar radiation database (*) PVGIS-SARAH
 Month* July Local time ()

On fixed plane:
 Irradiance
 Clear-sky irradiance
 Slope [°] ()
 Azimuth [°] ()

On sun-tracking plane:
 Irradiance
 Clear-sky irradiance

Temperature:
 Daily temperature profile

Address: [Go!](#) Lat/Lon: () [Go!](#) [Visualize results](#) [↓ csv](#) [↓ json](#)

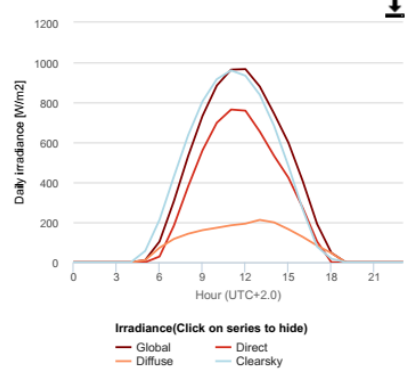
AVERAGE DAILY IRRADIANCE DATA: RESULTS

[Fixed-plane](#) [Tracking](#) [Temperature](#) [Info](#) [PDF](#)

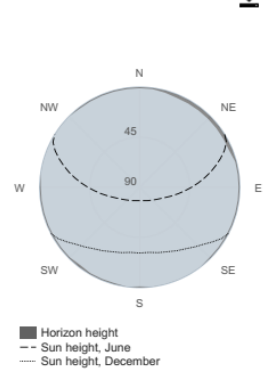
Summary

Provided inputs:
 Location [Lat/Lon]: 35.127, 33.376
 Horizon: Calculated
 Database used: PVGIS-SARAH
 Month: July

Daily average irradiance



Outline of horizon

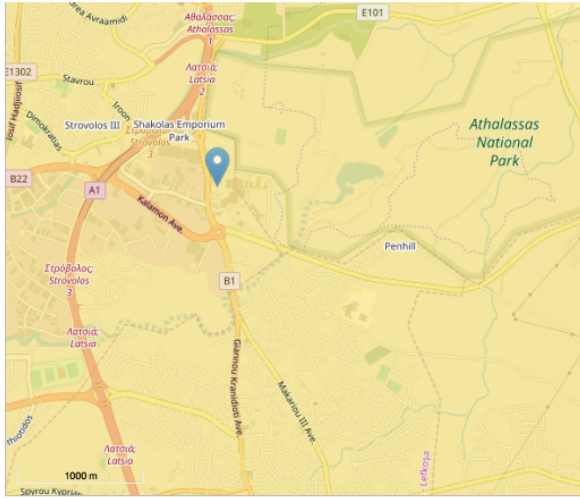


Last update: 15/10/2019 Top



PHOTOVOLTAIC GEOGRAPHICAL INFORMATION SYSTEM

European Commission (http://ec.europa.eu/index_en.htm) > EU Science Hub (https://ec.europa.eu/jrc/en/) > PVGIS (https://ec.europa.eu/jrc/en/pvgis) > Interactive tools (/pvg_tools/en/tools.html)



Cursor:
Selected: 35.127, 33.376
 Elevation: 177 (m)

Use terrain shadows:
 Calculated horizon ()
 Upload horizon file ()

Download buttons: [csv](#) [json](#)
 Choose file: [Choose file](#) No file chosen

AVERAGE DAILY IRRADIANCE DATA

Solar radiation database (*) PVGIS-SARAH

Month* August

UTC time ()
 Local time ()

On fixed plane:
 Irradiance
 Clear-sky irradiance
 Slope [°] ()
 Azimuth [°] ()

On sun-tracking plane:
 Irradiance
 Clear-sky irradiance

Temperature:
 Daily temperature profile

Address: [Go!](#) Lat/Lon: ([Go!](#) [Visualize results](#) [csv](#) [json](#)

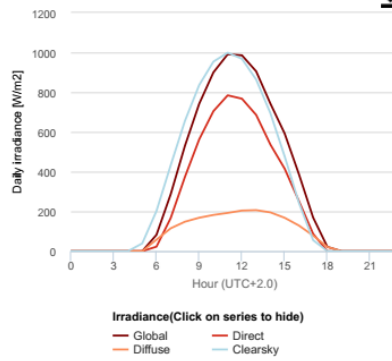
AVERAGE DAILY IRRADIANCE DATA: RESULTS

[Fixed-plane](#) [Tracking](#) [Temperature](#) [Info](#) [PDF](#)

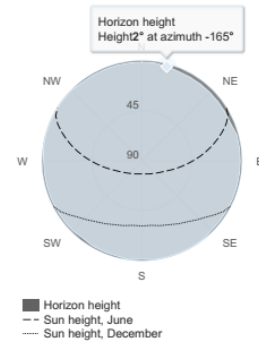
Summary

Provided inputs:
 Location [Lat/Lon]: 35.127, 33.376
 Horizon: Calculated
 Database used: PVGIS-SARAH
 Month: August

Daily average irradiance



Outline of horizon



Last update: 15/10/2019 Top

Appendix 5 – GlareGauge Assessment

Flight Path 1 (PV Array 1) GlareGauge Assessment



Demo Project NGH Helipad

Created May 1, 2021
Updated May 1, 2021
Time-step 10 minute(s)
Timezone offset UTC2
Site ID 53141.9547

Project type Demo
Project status: active



Misc. Analysis Settings

DNI: varies (1,000.0 W/m² peak)
Ocular transmission coefficient: 0.5
Pupil diameter: 0.002 m
Eye focal length: 0.017 m
Sun subtended angle: 9.3 mrad

Analysis Methodologies:
• Observation point: Version 2
• 2-Mile Flight Path: Version 2
• Route: Version 2

Summary of Results No glare predicted!

PV Name	Tilt deg	Orientation deg	"Green" Glare min	"Yellow" Glare min	Energy Produced kWh
PV array 1	32.0	180.0	0	0	1,681,000.0

Component Data

PV Array(s)

Total PV footprint area: 11,282 m²

Name: PV array 1
Description: FP1
Axis tracking: Fixed (no rotation)
Tilt: 32.0 deg
Orientation: 180.0 deg
Footprint area: 11,282 m²
Rater power: 700.0 kW
Panel material: Smooth glass with AR coating
Very reflectivity with sun position? Yes
Correlate slope error with surface type? Yes
Slope error: 8.43 mrad

Vertex	Latitude deg	Longitude deg	Ground elevation m	Height above ground m	Total elevation m
1	35.128735	33.374818	181.37	0.00	181.37
2	35.128525	33.375678	181.00	0.00	181.00
3	35.127244	33.375655	178.12	0.00	178.12
4	35.127279	33.374883	178.68	0.00	178.68



2-Mile Flight Path Receptor(s)

Name: FP 1
Description:
Threshold height: 15 m
Direction: 21.4 deg
Glide slope: 3.0 deg
Pilot view restricted? Yes
Vertical view restriction: 30.0 deg
Azimuthal view restriction: 90.0 deg

Point	Latitude deg	Longitude deg	Ground elevation m	Height above ground m	Total elevation m
Threshold	35.117042	33.378234	184.20	15.24	199.44
2-mile point	35.100130	33.365297	203.57	164.55	368.13



Route Receptor(s)

Name: Route 1
Route type Two-way
View angle: 50.0 deg



Vertex	Latitude	Longitude	Ground elevation	Height above ground	Total elevation
	deg	deg	m	m	m
1	33.727059	33.378223	184.18	0.00	184.18
2	33.128061	33.378634	185.79	0.00	185.79

Summary of PV Glare Analysis

PV configuration and total predicted glare

PV Name	Tilt	Orientation	"Green" Glare	"Yellow" Glare	Energy Produced	Data File
	deg	deg	min	min	kWh	
PV array 1	32.0	180.0	0	0	1,681,000.0	-

PV & Receptor Analysis Results

Results for each PV array and receptor

PV array 1 no glare found

Predicted energy output: 1,681,000.0 kWh (assuming sunny, clear skies)

Component	Green glare (min)	Yellow glare (min)
FP: FP 1	0	0
Route: Route 1	0	0

No glare found

Assumptions

- Times associated with glare are denoted in Standard time. For Daylight Savings, add one hour.
- Glare analyses do not account for physical obstructions between reflectors and receptors. This includes buildings, tree cover and geographic obstructions.
- Detailed system geometry is not rigorously simulated.
- The glare hazard determination relies on several approximations including observer eye characteristics, angle of view, and typical blink response time. Actual values and results may vary.
- The system output calculation is a DNI-based approximation that assumes clear, sunny skies year-round. It should not be used in place of more rigorous modeling methods.
- Several V1 calculations utilize the PV array centroid, rather than the actual glare spot location, due to algorithm limitations. This may affect results for large PV footprints. Additional analyses of array sub-sections can provide additional information on expected glare.
- The subtended source angle (glare spot size) is constrained by the PV array footprint size. Partitioning large arrays into smaller sections will reduce the maximum potential subtended angle, potentially impacting results if actual glare spots are larger than the sub-array size. Additional analyses of the combined area of adjacent sub-arrays can provide more information on potential glare hazards. (See previous point on related limitations.)
- Hazard zone boundaries shown in the Glare Hazard plot are an approximation and visual aid. Actual ocular impact outcomes encompass a continuous, not discrete, spectrum.
- Glare locations displayed on receptor plots are approximate. Actual glare-spot locations may differ.
- Glare vector plots are simplified representations of analysis data. Actual glare emanations and results may differ.
- Refer to the Help page for detailed assumptions and limitations not listed here.

Flight Path 2 (PV Array 1) GlareGauge Assessment



Demo Project NGH Helipad

Created May 1, 2021
Updated May 1, 2021
Time-step: 10 minute(s)
Timezone offset: UTC-7
Site ID: 53140.9547

Project type: Demo
Project status: active



Misc. Analysis Settings

DNI: varies (1,000.0 W/m² peak)
Ocular transmission coefficient: 0.5
Pupil diameter: 0.002 m
Eye focal length: 0.017 m
Sun subtended angle: 9.3 mrad

Analysis Methodologies:
• Observation point: Version 2
• 2-Mile Flight Path: Version 2
• Route: Version 2

Summary of Results No glare predicted!

PV Name	Tilt	Orientation	"Green" Glare	"Yellow" Glare	Energy Produced
	deg	deg	min	min	kWh
PV array 2	32.0	180.0	0	0	1,681,000.0

Component Data

PV Array(s)

Total PV footprint area: 11,262 m²

Name: PV array 2
Description: FP3
Axis tracking: Fixed (no rotation)
Tilt: 32.0 deg
Orientation: 180.0 deg
Footprint area: 11,262 m²
Rated power: 700.0 kW
Panel material: Smooth glass with AR coating
Vary reflectivity with sun position? Yes
Correlate slope error with surface type? Yes
Slope error: 8.43 mrad

Vertex	Latitude	Longitude	Ground elevation	Height above ground	Total elevation
	deg	deg	m	m	m
1	35.128735	33.374818	181.37	0.00	181.37
2	35.128525	33.375076	181.00	0.00	181.00
3	35.127244	33.375055	178.12	0.00	178.12
4	35.127279	33.374883	178.68	0.00	178.68



2-Mile Flight Path Receptor(s)

Name: FP 2
Description:
Threshold height: 15 m
Direction: 0.0 deg
Glide slope: 3.0 deg
Pilot view restricted? Yes
Vertical view restriction: 30.0 deg
Azimuthal view restriction: 50.0 deg

Point	Latitude	Longitude	Ground elevation	Height above ground	Total elevation
	deg	deg	m	m	m
Threshold	35.127366	33.378509	183.08	15.24	198.32
2-mile point	35.098454	33.378509	205.82	161.18	367.01



Route Receptor(s)

Name: Route 1
Route type Two-way
View angle: 50.0 deg



Vertex	Latitude	Longitude	Ground elevation	Height above ground	Total elevation
	deg	deg	m	m	m
1	35.128016	33.378509	185.86	0.00	185.86
2	35.127364	33.378509	183.07	0.00	183.07

Summary of PV Glare Analysis

PV configuration and total predicted glare

PV Name	Tilt	Orientation	"Green" Glare	"Yellow" Glare	Energy Produced	Data File
	deg	deg	min	min	kWh	
PV array 2	32.0	180.0	0	0	1,681,000.0	-

PV & Receptor Analysis Results

Results for each PV array and receptor

PV array 2 no glare found

Predicted energy output: 1,681,000.0 kWh (assuming sunny, clear skies)

Component	Green glare (min)	Yellow glare (min)
FP: FP 2	0	0
Route: Route 1	0	0

No glare found

Assumptions

- Times associated with glare are denoted in Standard time. For Daylight Savings, add one hour.
- Glare analyses do not account for physical obstructions between reflectors and receptors. This includes buildings, tree cover and geographic obstructions.
- Detailed system geometry is not rigorously simulated.
- The glare hazard determination relies on several approximations including observer eye characteristics, angle of view, and typical blink response time. Actual values and results may vary.
- The system output calculation is a DNI-based approximation that assumes clear, sunny skies year-round. It should not be used in place of more rigorous modeling methods.
- Several VI calculations utilize the PV array centroid, rather than the actual glare spot location, due to algorithm limitations. This may affect results for large PV footprints. Additional analyses of array sub-sections can provide additional information on expected glare.
- The subtended source angle (glare spot size) is constrained by the PV array footprint size. Partitioning large arrays into smaller sections will reduce the maximum potential subtended angle, potentially impacting results if actual glare spots are larger than the sub-array size. Additional analyses of the combined areas of adjacent sub-arrays can provide more information on potential glare hazards. (See previous point on related limitations.)
- Hazard zone boundaries shown in the Glare Hazard plot are an approximation and visual aid. Actual ocular impact outcomes encompass a continuous, not discrete, spectrum.
- Glare locations displayed on receptor plots are approximate. Actual glare-spot locations may differ.
- Glare vector plots are simplified representations of analysis data. Actual glare emissions and results may differ.
- Refer to the Help page for detailed assumptions and limitations not listed here.

Flight Path 3 (PV Array 1) GlareGauge Assessment



Demo Project NGH Helipad

Created May 1, 2021
Updated May 1, 2021
Time-step: 10 minute(s)
Timezone offset UTC2
Site ID: 53136.9502

Project type: Demo
Project status: active



Misc. Analysis Settings

DNI: varies (1,000.0 W/m² peak)
Ocular transmission coefficient: 0.5
Pupil diameter: 0.002 m
Eye focal length: 0.017 m
Sun subtended angle: 9.3 mrad

Analysis Methodologies:

- Observation point: Version 2
- 2-Mile Flight Path: Version 2
- Route: Version 2

Summary of Results Glare with potential for temporary after-image predicted

PV Name	Tilt	Orientation	"Green" Glare	"Yellow" Glare	Energy Produced
	deg	deg	min	min	kWh
PV array 1	32.0	180.0	152	365	-

Component Data

PV Array(s)

Total PV footprint area: 10,519 m²

Name: PV array 1
Description: FP3
Axis tracking: Fixed (no rotation)
Tilt: 32.0 deg
Orientation: 180.0 deg
Footprint area: 10,519 m²
Rated power: -
Panel material: Smooth glass with AR coating
Very reflectivity with sun position? Yes
Correlate slope error with surface type? Yes
Slope error: 8.43 mrad

Vertex	Latitude	Longitude	Ground elevation	Height above ground	Total elevation
	deg	deg	m	m	m
1	35.127344	33.374938	178.82	0.00	178.82
2	35.127326	33.375710	179.56	0.00	179.56
3	35.128554	33.375796	181.05	0.00	181.05
4	35.128600	33.374938	181.18	0.00	181.18



2-Mile Flight Path Receptor(s)

Name: FP 1
Description:
Threshold height: 15 m
Direction: 342.5 deg
Glide slope: 3.0 deg
Pilot view restricted? Yes
Vertical view restriction: 30.0 deg
Azimuthal view restriction: 50.0 deg

Point	Latitude	Longitude	Ground elevation	Height above ground	Total elevation
	deg	deg	m	m	m
Threshold	35.126852	33.378907	183.36	15.24	198.60
2-mile point	35.099282	33.389568	200.88	166.40	367.28



Route Receptor(s)

Name: Route 3
Route type Two-way
View angle: 50.0 deg



Official Demo Use Only

Vertex	Latitude deg	Longitude deg	Ground elevation m	Height above ground m	Total elevation m
1	35.126843	33.378529	183.34	0.00	183.34
2	35.128028	33.378553	185.67	0.00	185.67

Summary of PV Glare Analysis

PV configuration and total predicted glare

PV Name	Tilt deg	Orientation deg	"Green" Glare min	"Yellow" Glare min	Energy Produced kWh	Data File
PV array 1	32.0	180.0	152	365	-	-

Distinct glare per month

Excludes overlapping glare from PV array for multiple receptors at matching time(s)

PV	Jan	Feb	Mar	Apr	May	Jun	Jul	Aug	Sep	Oct	Nov	Dec
pv-array-1 (green)	0	0	0	0	35	60	43	5	0	0	0	0
pv-array-1 (yellow)	0	0	0	4	70	60	67	34	0	0	0	0

PV & Receptor Analysis Results

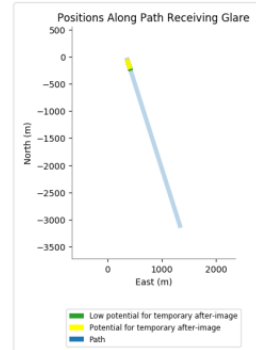
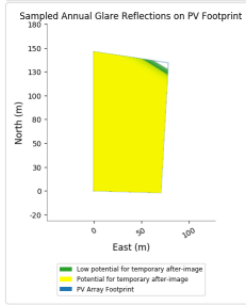
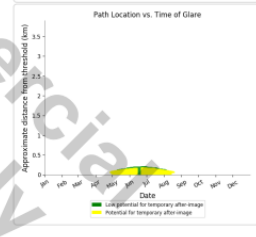
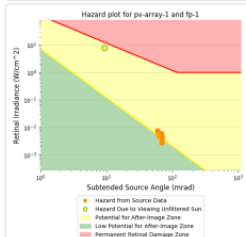
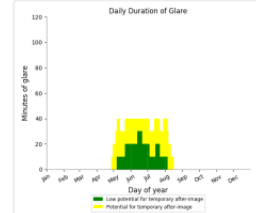
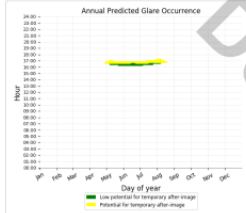
Results for each PV array and receptor

PV array 1 potential temporary after-image

Component	Green glare (min)	Yellow glare (min)
FP: FP 1	152	226
Route: Route 3	0	139

PV array 1 - Receptor (FP 1)

PV array is expected to produce the following glare for observers on this flight path:
 • 152 minutes of "green" glare with low potential to cause temporary after-image.
 • 226 minutes of "yellow" glare with potential to cause temporary after-image.



Flight Path 1(PV Array 2) GlareGauge Assessment



Demo Project Untitled

Created May 2, 2021
Updated May 2, 2021
Time-step: 10 minute(s)
Timezone offset: UTC2
Site ID: 53143.9549

Project type: Demo
Project status: active



Misc. Analysis Settings

DNI: varies (1,000.0 W/m² peak)
Ocular transmission coefficient: 0.5
Pupil diameter: 0.002 m
Eye focal length: 0.017 m
Sun subtended angle: 9.3 mrad

Analysis Methodologies:
• Observation point: Version 2
• 2-Mile Flight Path: Version 2
• Router: Version 2

Summary of Results No glare predicted!

PV Name	Tilt deg	Orientation deg	"Green" Glare min	"Yellow" Glare min	Energy Produced kWh
PV array 2	32.0	180.0	0	0	583,200.0

Component Data

PV Array(s)

Total PV footprint area: 4,422 m²

Name: PV array 2
Description: FP1
Axis tracking: Fixed (no rotation)
Tilt: 32.0 deg
Orientation: 180.0 deg
Footprint area: 4,422 m²
Rated power: 243.0 kW
Panel material: Smooth glass with AR coating
Vary reflectivity with sun position? Yes
Correlate slope error with surface type? Yes
Slope error: 8.43 mrad

Vertex	Latitude deg	Longitude deg	Ground elevation m	Height above ground m	Total elevation m
1	35.120907	33.374990	177.65	0.00	177.65
2	35.120907	33.375462	177.69	0.00	177.69
3	35.120924	33.375419	176.14	0.00	176.14
4	35.120969	33.375161	175.87	0.00	175.87
5	35.126257	33.374925	176.56	0.00	176.56



2-Mile Flight Path Receptor(s)

Name: FP 1
Description:
Threshold height: 15 m
Direction: 21.0 deg
Glide slope: 3.0 deg
Pilot view restriction? Yes
Vertical view restriction: 30.0 deg
Azimuthal view restriction: 90.0 deg

Point	Latitude deg	Longitude deg	Ground elevation m	Height above ground m	Total elevation m
Threshold	35.127100	33.378187	184.16	15.24	199.40
2-mile point	35.100107	33.365603	203.19	164.90	368.09



Route Receptor(s)

Name: Route 1
Route type Two-way
View angle: 90.0 deg



Vertex	Latitude	Longitude	Ground elevation	Height above ground	Total elevation
	deg	deg	m	m	m
1	35.127117	33.378185	184.16	0.00	184.16
2	35.128095	33.379530	185.83	0.00	185.83

Summary of PV Glare Analysis

PV configuration and total predicted glare

PV Name	Tilt	Orientation	"Green" Glare	"Yellow" Glare	Energy Produced	Data File
	deg	deg	min	min	kWh	
PV array 2	32.0	180.0	0	0	583,200.0	-

PV & Receptor Analysis Results

Results for each PV array and receptor

PV array 2 no glare found

Predicted energy output: 583,200.0 kWh (assuming sunny, clear skies)

Component	Green glare (min)	Yellow glare (min)
FP: FP 1	0	0
Route: Route 1	0	0

No glare found

Assumptions

- Times associated with glare are denoted in Standard time. For Daylight Savings, add one hour.
- Glare analyses do not account for physical obstructions between reflectors and receptors. This includes buildings, tree cover and geographic obstructions.
- Detailed system geometry is not rigorously simulated.
- The glare hazard determination relies on several approximations including observer eye characteristics, angle of view, and typical blink response time. Actual values and results may vary.
- The system output calculation is a DN-biased approximation that assumes clear, sunny skies year-round. It should not be used in place of more rigorous modeling methods.
- Several V1 calculations utilize the PV array centroid, rather than the actual glare spot location, due to algorithm limitations. This may affect results for large PV footprints. Additional analyses of array sub-sections can provide additional information on expected glare.
- The subtended source angle (glare spot size) is constrained by the PV array footprint size. Partitioning large arrays into smaller sections will reduce the maximum potential subtended angle, potentially impacting results if actual glare spots are larger than the sub-array size.
- Additional analyses of the combined area of adjacent sub-arrays can provide more information on potential glare hazards. (See previous point on related limitations.)
- Hazard zone boundaries shown in the Glare Hazard plot are an approximation and visual aid. Actual ocular impact outcomes encompass a continuous, not discrete, spectrum.
- Glare locations displayed on receptor plots are approximate. Actual glare-spot locations may differ.
- Glare vector plots are simplified representations of analysis data. Actual glare emanations and results may differ.
- Refer to the Help page for detailed assumptions and limitations not listed here.

Flight Path 2 (PV Array 2) GlareGauge Assessment



Demo Project Untitled

Created May 2, 2021
Updated May 2, 2021
Time-step: 10 minute(s)
Timezone offset UTCZ
Site ID 53144.9549

Project type Demo
Project status: active



Misc. Analysis Settings

DNI: varies (1,000.0 W/m² peak)
Ocular transmission coefficient: 0.5
Pupil diameter: 6.002 m
Eye focal length: 0.017 m
Sun subtended angle: 9.3 mrad

Analysis Methodologies:

- Observation point: Version 2
- 2-Mile Flight Path: Version 2
- Route: Version 2

Summary of Results No glare predicted!

PV Name	Tilt deg	Orientation deg	"Green" Glare min	"Yellow" Glare min	Energy Produced kWh
PV array 2	32.0	180.0	0	0	583,200.0

Component Data

PV Array(s)

Total PV footprint area: 4,422 m²

Name: PV array 2
Description: FP2
Axis tracking: Fixed (no rotation)
Tilt: 32.0 deg
Orientation: 180.0 deg
Footprint area: 4,422 m²
Rated power: 243.0 kW
Panel material: Smooth glass with AR coating
Vary reflectivity with sun position? Yes
Concrete slope error with surface type? Yes
Slope error: 8.43 mrad

Vertex	Latitude deg	Longitude deg	Ground elevation m	Height above ground m	Total elevation m
1	35.126907	33.374990	177.65	0.00	177.65
2	35.126907	33.375462	177.69	0.00	177.69
3	35.125924	33.375419	176.14	0.00	176.14
4	35.125959	33.375161	175.87	0.00	175.87
5	35.126257	33.374925	176.56	0.00	176.56



2-Mile Flight Path Receptor(s)

Name: FP 1
Description:
Threshold height: 15 m
Direction: 0.0 deg
Glide slope: 3.0 deg
Pilot view restricted? Yes
Vertical view restriction: 30.0 deg
Azimuthal view restriction: 90.0 deg

Point	Latitude deg	Longitude deg	Ground elevation m	Height above ground m	Total elevation m
Threshold	35.126626	33.378480	183.70	15.24	198.94
2-mile point	35.097713	33.378480	204.76	162.86	367.63



Route Receptor(s)

Name: Route 2
Route type: Two-way
View angle: 50.0 deg



Vertex	Latitude	Longitude	Ground elevation	Height above ground	Total elevation
	deg	deg	m	m	m
1	35.72591	33.378437	183.61	0.00	183.61
2	35.72830	33.378394	185.55	0.00	185.55

Summary of PV Glare Analysis

PV configuration and total predicted glare

PV Name	Tilt	Orientation	"Green" Glare	"Yellow" Glare	Energy Produced	Data File
	deg	deg	min	min	kWh	
PV array 2	32.0	180.0	0	0	583,200.0	-

PV & Receptor Analysis Results

Results for each PV array and receptor

PV array 2 no glare found

Predicted energy output: 583,200.0 kWh (assuming sunny, clear skies)

Component	Green glare (min)	Yellow glare (min)
FP: FP 1	0	0
Route: Route 2	0	0

No glare found

Assumptions

- Times associated with glare are denoted in Standard time. For Daylight Savings, add one hour.
- Glare analyses do not account for physical obstructions between reflectors and receptors. This includes buildings, tree cover and geographic obstructions.
- Detailed system geometry is not rigorously simulated.
- The glare hazard determination relies on several approximations including observer eye characteristics, angle of view, and typical blink response time. Actual values and results may vary.
- The system output calculation is a DNb-based approximation that assumes clear, sunny skies year-round. It should not be used in place of more rigorous modeling methods.
- Several VI calculations utilize the PV array centroid, rather than the actual glare spot location, due to algorithm limitations. This may affect results for large PV footprints. Additional analyses of array sub-sections can provide additional information on expected glare.
- The subtended source angle (glare spot size) is constrained by the PV array footprint size. Partitioning large arrays into smaller sections will reduce the maximum potential subtended angle, potentially impacting results if actual glare spots are larger than the sub-array size.
- Additional analyses of the combined area of adjacent sub-arrays can provide more information on potential glare hazards. (See previous point on related limitations.)
- Hazard zone boundaries shown in the Glare Hazard plot are an approximation and visual aid. Actual ocular impact outcomes encompass a continuous, not discrete, spectrum.
- Glare locations displayed on receptor plots are approximate. Actual glare-spot locations may differ.
- Glare vector plots are simplified representations of glare analysis data. Actual glare emanations and results may differ.
- Refer to the Help page for detailed assumptions and limitations not listed here.

Flight Path 3 (PV Array 2) GlareGauge Assessment



Demo Project Untitled

Created May 2, 2021
Updated May 2, 2021
Time-step: 10 minutes
Timezone offset: UTC-2
Site ID: 53145.9549

Project type: Demo
Project status: active



Misc. Analysis Settings

DNI: varies (1,000.0 W/m² peak)
Ocular transmission coefficient: 0.5
Pupil diameter: 0.002 m
Eye focal length: 0.017 m
Sun subtended angle: 9.3 mrad

Analysis Methodologies:
• Observation point: Version 2
• 2-Mile Flight Path: Version 2
• Route: Version 2

Summary of Results

Glare with low potential for temporary after-image predicted

PV Name	Tilt	Orientation	"Green" Glare	"Yellow" Glare	Energy Produced
	deg	deg	min	min	kWh
PV array 2	32.0	180.0	391	0	583,200.0

Component Data

PV Array(s)

Total PV footprint area: 4,422 m²

Name: PV array 2
Description: FP3
Axis tracking: Fixed (no rotation)
Tilt: 32.0 deg
Orientation: 180.0 deg
Footprint area: 4,422 m²
Rated power: 243.0 kW
Panel material: Smooth glass with AR coating
Very reflective with sun position? Yes
Correlate slope error with surface type? Yes
Slope error: 8.43 mrad

Vertex	Latitude	Longitude	Ground elevation	Height above ground	Total elevation
	deg	deg	m	m	m
1	35.126907	33.374990	177.65	0.00	177.65
2	35.126907	33.375462	177.69	0.00	177.69
3	35.125024	33.375419	176.14	0.00	176.14
4	35.126959	33.375161	175.87	0.00	175.87
5	35.126257	33.374925	176.56	0.00	176.56



2-Mile Flight Path Receptor(s)

Name: FP 3
Description:
Threshold height: 15 m
Direction: 342.0 deg
Glide slope: 3.0 deg
Pilot view restricted? Yes
Vertical view restriction: 30.0 deg
Azimuthal view restriction: 90.0 deg

Point	Latitude	Longitude	Ground elevation	Height above ground	Total elevation
	deg	deg	m	m	m
Threshold	35.126801	33.378781	183.56	15.24	198.80
2-mile point	35.099304	33.389717	200.82	166.87	367.68



Route Receptor(s)

Name: Route 3
 Route type: Two-way
 View angle: 50.0 deg



Vertex	Latitude	Longitude	Ground elevation	Height above ground	Total elevation
	deg	deg	m	m	m
1	35.126907	33.378781	183.46	0.00	183.46
2	35.127986	33.378437	185.45	0.00	185.45

Summary of PV Glare Analysis

PV configuration and total predicted glare

PV Name	Tilt deg	Orientation deg	"Green" Glare min	"Yellow" Glare min	Energy Produced kWh	Data File
PV array 2	32.0	180.0	391	0	583,200.0	-

Distinct glare per month

Excludes overlapping glare from PV array for multiple receptors at matching time(s)

PV	Jan	Feb	Mar	Apr	May	Jun	Jul	Aug	Sep	Oct	Nov	Dec
pv-array-2 (green)	0	0	0	10	112	104	116	49	0	0	0	0
pv-array-2 (yellow)	0	0	0	0	0	0	0	0	0	0	0	0

PV & Receptor Analysis Results

Results for each PV array and receptor

PV array 2 - low potential for temporary after-image

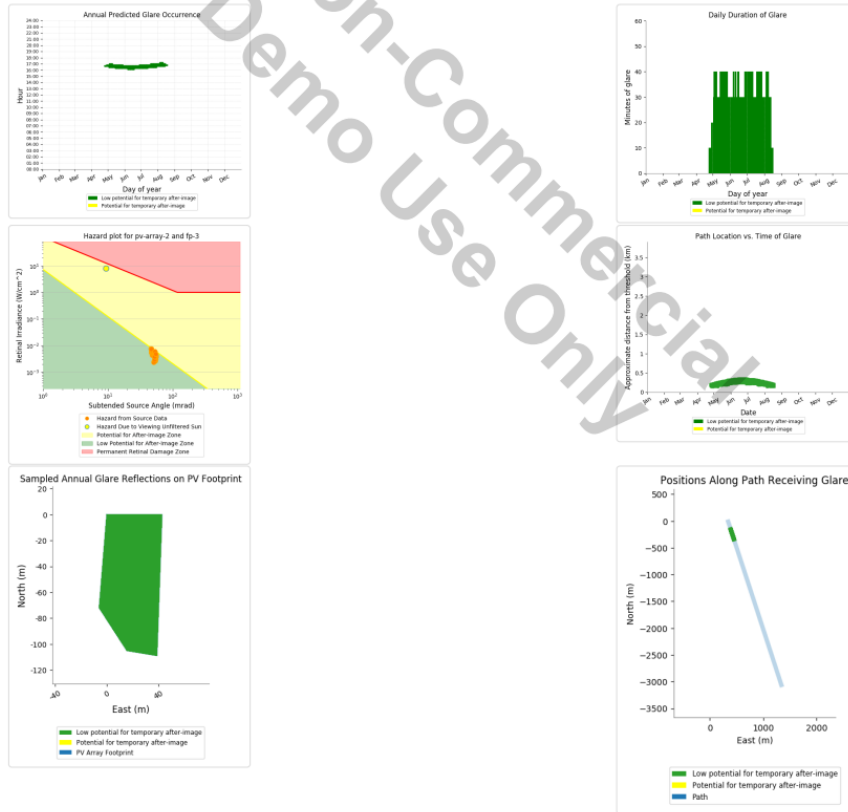
Predicted energy output: 583,200.0 kWh (assuming sunny, clear skies)

Component	Green glare (min)	Yellow glare (min)
FP: FP 3	391	0
Route: Route 3	0	0

PV array 2 - Receptor (FP 3)

PV array is expected to produce the following glare for observers on this flight path:

- 391 minutes of "green" glare with low potential to cause temporary after-image.
- 0 minutes of "yellow" glare with potential to cause temporary after-image.



PV array 2 - Route Receptor (Route 3)

No glare found

Assumptions

- Times associated with glare are denoted in Standard time. For Daylight Savings, add one hour.
- Glare analyses do not account for physical obstructions between reflectors and receptors. This includes buildings, tree cover and geographic obstructions.
- Detailed system geometry is not rigorously simulated.
- The glare hazard determination relies on several approximations including observer eye characteristics, angle of view, and typical blink response time. Actual values and results may vary.
- The system output calculation is a DNI-based approximation that assumes clear, sunny skies year-round. It should not be used in place of more rigorous modeling methods.
- Several VI calculations utilize the PV array centroid, rather than the actual glare spot location, due to algorithm limitations. This may affect results for large PV footprints. Additional analyses of array sub-sections can provide additional information on expected glare.
- The subtended source angle (glare spot size) is constrained by the PV array footprint size. Partitioning large arrays into smaller sections will reduce the maximum potential subtended angle, potentially impacting results if actual glare spots are larger than the sub-array size.
- Additional analyses of the combined area of adjacent sub-arrays can provide more information on potential glare hazards. (See previous point on related limitations.)
- Hazard zone boundaries shown in the Glare Hazard plot are an approximation and visual aid. Actual ocular impact outcomes encompass a continuous, not discrete, spectrum.
- Glare locations displayed on receptor plots are approximate. Actual glare-spot locations may differ.
- Glare vector plots are simplified representations of analysis data. Actual glare emanations and results may differ.
- Refer to the Help page for detailed assumptions and limitations not listed here.

Flight Path 3 (PV Array 1) GlareGauge Assessment – Mitigation Assessment



ForgeSolar

Demo Project NGH Helipad

Created May 1, 2021
Updated May 1, 2021
Time-step 10 minutes
Timezone offset UTC
Site ID 53138.9562

Project type Demo
Project status: active



Misc. Analysis Settings

DNI: varies (1,000.0 W/m² peak)
Ocular transmission coefficient: 0.5
Pupil diameter: 6.002 m
Eye focal length: 0.017 m
Sun subtended angle: 9.3 mrad

Analysis Methodologies:
• Observation point: Version 2
• 2-Mile Flight Path: Version 2
• Route: Version 2

Summary of Results Glare with low potential for temporary after-image predicted

PV Name	Tilt	Orientation	"Green" Glare	"Yellow" Glare	Energy Produced
	deg	deg	min	min	kWh
PV array 1	32.0	180.0	4,663	0	-

Component Data

PV Array(s)

Total PV footprint area: 10,519 m²

Name: PV array 1
Description: FP3
Axis tracking: Fixed (no rotation)
Tilt: 32.0 deg
Orientation: 180.0 deg
Footprint area: 10,519 m²
Rated power: -
Panel material: Deeply textured glass
Vary reflectivity with sun position? Yes
Correlate slope error with surface type? Yes
Slope error: 82.6 mrad

Vertex	Latitude	Longitude	Ground elevation	Height above ground	Total elevation
	deg	deg	m	m	m
1	35.127344	33.374938	178.82	0.00	178.82
2	35.127326	33.375710	179.56	0.00	179.56
3	35.128554	33.375796	181.05	0.00	181.05
4	35.128600	33.374938	181.18	0.00	181.18



2-Mile Flight Path Receptor(s)

Name: FP 1
Description:
Threshold height: 15 m
Direction: 342.5 deg
Glide slope: 3.0 deg
Pilot view restricted? Yes
Vertical view restriction: 30.0 deg
Azimuthal view restriction: 50.0 deg

Point	Latitude	Longitude	Ground elevation	Height above ground	Total elevation
	deg	deg	m	m	m
Threshold	35.120852	33.378907	183.36	15.24	198.60
2-mile point	35.099282	33.389568	200.88	166.40	367.28



Route Receptor(s)

Name: Route 3
Route type: Two-way
View angle: 50.0 deg



Vertex	Latitude	Longitude	Ground elevation	Height above ground	Total elevation
	deg	deg	m	m	m
1	35.126843	33.378929	183.34	0.00	183.34
2	35.128028	33.378553	185.67	0.00	185.67

Summary of PV Glare Analysis

PV configuration and total predicted glare

PV Name	Tilt	Orientation	"Green" Glare	"Yellow" Glare	Energy Produced	Data File
	deg	deg	min	min	kWh	
PV array 1	32.0	180.0	4,663	0	-	-

Distinct glare per month

Excludes overlapping glare from PV array for multiple receptors at matching time(s)

PV	Jan	Feb	Mar	Apr	May	Jun	Jul	Aug	Sep	Oct	Nov	Dec
pv-array-1 (green)	0	77	359	463	560	591	587	503	414	169	4	0
pv-array-1 (yellow)	0	0	0	0	0	0	0	0	0	0	0	0

PV & Receptor Analysis Results

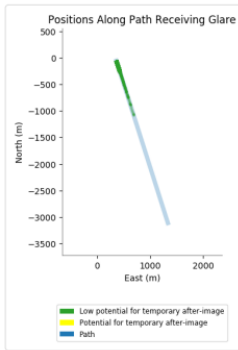
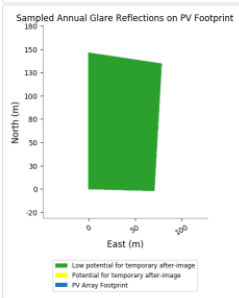
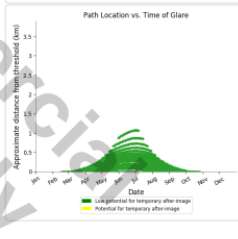
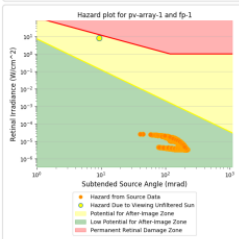
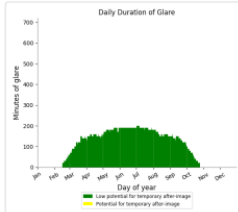
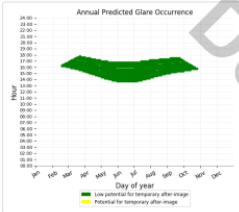
Results for each PV array and receptor

PV array 1 low potential for temporary after-image

Component	Green glare (min)	Yellow glare (min)
FP: FP 1	3628	0
Route: Route 3	1035	0

PV array 1 - Receptor (FP 1)

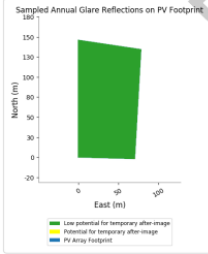
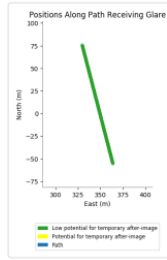
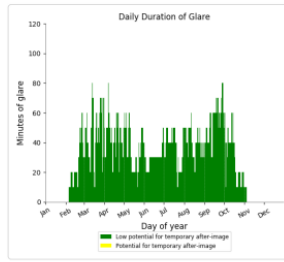
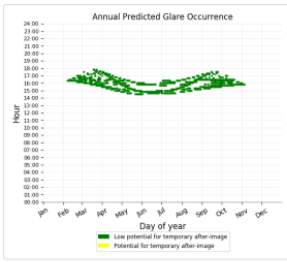
PV array is expected to produce the following glare for observers on this flight path:
 • 3,628 minutes of "green" glare with low potential to cause temporary after-image.
 • 0 minutes of "yellow" glare with potential to cause temporary after-image.



PV array 1 - Route Receptor (Route 3)

PV array is expected to produce the following glare for receptors at this location:

- 1,035 minutes of "green" glare with low potential to cause temporary after-image.
- 0 minutes of "yellow" glare with potential to cause temporary after-image.



Assumptions

- Times associated with glare are denoted in Standard time. For Daylight Savings, add one hour.
- Glare analyses do not account for physical obstructions between reflectors and receptors. This includes buildings, tree cover and geographic obstructions.
- Detailed system geometry is not rigorously simulated.
- The glare hazard determination relies on several approximations including observer eye characteristics, angle of view, and typical blink response time. Actual values and results may vary.
- The system output calculation is a DNb-based approximation that assumes clear, sunny skies year-round. It should not be used in place of more rigorous modeling methods.
- Several V1 calculations utilize the PV array centroid, rather than the actual glare spot location, due to algorithm limitations. This may affect results for large PV footprints. Additional analyses of array sub-sections can provide additional information on expected glare.
- The subtended source angle (glare spot size) is constrained by the PV array footprint size. Partitioning large arrays into smaller sections will reduce the maximum potential subtended angle, potentially impacting results if actual glare spots are larger than the sub-array size. Additional analyses of the combined area of adjacent sub-arrays can provide more information on potential glare hazards. (See previous point on related limitations.)
- Hazard zone boundaries shown in the Glare Hazard plot are an approximation and visual aid. Actual ocular impact outcomes encompass a continuous, not discrete, spectrum.
- Glare locations displayed on receptor plots are approximate. Actual glare-spot locations may differ.
- Glare vector plots are simplified representations of analysis data. Actual glare emanations and results may differ.
- Refer to the [Help](#) page for detailed assumptions and limitations not listed here.